NSWC TR 85-380



# STATIC DIELECTRIC BREAKDOWN STRENGTH OF CONDENSED HETEROGENEOUS HIGH EXPLOSIVES

BY RICHARD J. LEE

RESEARCH AND TECHNOLOGY DEPARTMENT

JUNE 1987





NAVAL SURFACE WEAPONS CENTER

Dahlgren, Virginia 22448-5000 • Silver Spring, Maryland 20903-5000

# REPORT DOCUMENTATION PAGE

| | |
|---|---|
| 1a. REPORT SECURITY CLASSIFICATION<br>UNCLASSIFIED | 1b RESTRICTIVE MARKINGS AD-A191 033 |
| 2a SECURITY CLASSIFICATION AUTHORITY | 3. DISTRIBUTION / AVAILABILITY OF REPORT<br>Approved for public release; distribution is unlimited. |
| 2b DECLASSIFICATION / DOWNGRADING SCHEDULE | |
| 4. PERFORMING ORGANIZATION REPORT NUMBER(S)<br>NSWC TR 85-380 | 5 MONITORING ORGANIZATION REPORT NUMBER(S) |
| 6a NAME OF PERFORMING ORGANIZATION<br>NAVAL SURFACE WEAPONS CENTER<br>6b OFFICE SYMBOL (*If applicable*)<br>R13 | 7a NAME OF MONITORING ORGANIZATION |
| 6c. ADDRESS (*City, State, and ZIP Code*)<br>10901 New Hampshire Avenue<br>White Oak, Silver Spring, MD 20903-5000 | 7b. ADDRESS (*City, State, and ZIP Code*) |
| 8a NAME OF FUNDING / SPONSORING ORGANIZATION<br>OFFICE OF NAVAL RESEARCH<br>8b OFFICE SYMBOL (*If applicable*)<br>01124 | 9 PROCUREMENT INSTRUMENT IDENTIFICATION NUMBER |
| 8c. ADDRESS (*City, State, and ZIP Code*)<br>Arlington, VA 22217-5000 | 10 SOURCE OF FUNDING NUMBERS<br>PROGRAM ELEMENT NO. 62314N; PROJECT NO. RJ14E31; TASK NO NS3A; WORK UNIT ACCESSION NO. |

11. TITLE (*Include Security Classification*)

Static Dielectric Breakdown Strength of Condensed Heterogeneous High Explosives

12. PERSONAL AUTHOR(S)
LEE, R. J.

| 13a. TYPE OF REPORT | 13b TIME COVERED | 14. DATE OF REPORT (*Year, Month, Day*) | 15 PAGE COUNT |
|---|---|---|---|
| | FROM 10/84 TO 9/85 | 1987/June | 55 |

16. SUPPLEMENTARY NOTATION

| 17 COSATI CODES | | | 18 SUBJECT TERMS (*Continue on reverse if necessary and identify by block number*) |
|---|---|---|---|
| FIELD | GROUP | SUB-GROUP | Dielectric Breakdown, Partial Discharge Activity, Plastic Bonded Explosives, Shielded Triple Junctions |
| 19 | 01 | | |
| 20 | 03 | | |

19 ABSTRACT (*Continue on reverse if necessary and identify by block number*)

A new method of obtaining static dielectric breakdown strength data is reported. The breakdown strengths of plastic bonded explosives have been obtained using this method.

The theory of dielectric breakdown in solid materials, including explosives, is presented. The difficulties associated with the measurement of dielectric breakdown strengths are then analyzed in detail, and using this analysis, a new test method is described. (Keywords)

Dielectric breakdown results are provided for PBX-9404-03 (13.1 kV/mm), PBX-9501 (14.3 kV/mm), PBX-9502 (40 kV/mm), PBXW-108(I) (21.7 kV/mm), and Dupont's Detasheet Type CI (16.1 kV/mm) by E. I. duPont de Nemours & Company. These data are then critically analyzed and recommendations for future improvement are provided.

| 20 DISTRIBUTION / AVAILABILITY OF ABSTRACT | 21. ABSTRACT SECURITY CLASSIFICATION |
|---|---|
| ☐ UNCLASSIFIED/UNLIMITED ☑ SAME AS RPT ☐ DTIC USERS | UNCLASSIFIED |
| 22a. NAME OF RESPONSIBLE INDIVIDUAL<br>RICHARD J. LEE | 22b TELEPHONE (*Include Area Code*)<br>202-394-1530 / 22c. OFFICE SYMBOL<br>R13 |

# FOREWORD

This report describes the measurement of dielectric breakdown strengths for five plastic bonded explosives. These data are required for an understanding of the mechanisms of the electrostatic ignition of explosives and the coupling of electromagnetic energy to explosives. The measurements were obtained with a new test method which is also described.

The theory of static dielectric breakdown in solids is introduced, followed by the difficulties of measuring dielectric strengths. The solutions to these problems are addressed in the description of the test apparatus and procedures.

Static dielectric breakdown strengths are: PBX-9404-03 (13.1 kV/mm), PBX-9502 (40 kV/mm), PBXW-108(I) (21.7 kV/mm), and Detasheet Type C[1] (E. I. duPont de Nemours & Company Detasheet "C" Flexible Explosive) (16.1 kV/mm). The results demonstrate that the insulating properties of these explosives compare favorably with inert insulators such as polyethylene (18 kV/mm). These results also indicate that the dielectric strengths for composite explosives are strongly dependent on morphology.

This work was performed under the 6.1 Energy Coupling Program which is funded by the Naval Sea Systems Command under P. E. 61152N, SR 024-03.

The author wishes to acknowledge the assistance of Douglas G. Tasker and Jerry W. Forbes for many helpful discussions; Herman Gillum and Paul Gustavson for assisting in performing the tests; and Bill Freeman and John Roscher for their expertise in manufacturing the test cells.

Approved by:

Kurt F. Mueller

KURT F. MUELLER, Head
Energetic Materials Division

CONTENTS

CONTENTS (Cont.)

## ILLUSTRATIONS



## TABLES

# CHAPTER 1

## INTRODUCTION

This report describes the measurement of dielectric breakdown strengths for five plastic bonded explosives: PBX-9404-03, PBX-9501, PBX-9502, PBXW-108(I), and Dupont's Detasheet Type C (E.I. duPont de Nemours & Company Deta Sheet "C" Flexible Explosive).[1] These materials represent composites of the following explosives: HMX, TATB, RDX, and PETN. In order to make conclusions about dielectric breakdown in explosive compositions, various parameters of these materials (composition, morphology, density) are compared for 1 mm thick samples. Critical field strengths (the electric field strength at breakdown) are given for PBXW-108(I) for a range of thicknesses from 1 to 5 mm.

These data are required for understanding electrostatic ignition of explosives. Present electrostatic discharge (ESD) safety qualification tests are performed on explosive powders. The dielectric strengths for these powders are poor, thus allowing operation of these tests at relatively low voltages (5 to 7.5 kV). However, recent interest has been focused on ESD ignition for solid propellants. It is expected that this work will carry over to explosives. Therefore, to calculate the possibility of ESD ignition and perform capacitive discharge tests on these solids, an understanding of dielectric breakdown is required.

These data are also required to establish possible candidates for studying the coupling of electromagnetic energy to explosives.[3] To obtain efficient energy deposition to the detonation, large electric field strengths are required across the unreacted explosive. Therefore, it is necessary to use explosives which possess relatively high dielectric strengths.

Dielectric breakdown has not been studied as extensively for explosives as it has for other insulators. Therefore, theories on breakdown in reactive media have been modeled after those for non-reactive media.[4,5,6] The problem for explosive materials is complicated since they are non-homogeneous containing explosive crystals and binder systems. This constitutes a sea of regions with different density, dielectric constant, and dielectric strength. Despite this complication, it is necessary to understand the breakdown mechanisms for inerts to understand how they may differ for explosives.

The difference in breakdown for explosives may be a variation of the partial discharge mechanism adopted for inert insulators. Air voids existing in a material constitute a non-homogeneity with the aforementioned differences. A large fraction of the applied voltage appears across these voids due to capacitive division established between regions of differing dielectric constants. Partial discharges (discharges not bridging the entire gap) occur in these voids when the dielectric strength of the air gap formed by the void is exceeded. These discharges ultimately lead to catastrophic failure as described in Chapter 2.

At present, there is not enough experimental data to determine a proper breakdown model for explosives. Furthermore, these data, including this report, are still preliminary. The problems involved in these experiments are just being realized in the explosives community. There is a host of parameters that can dominate the experimental results (electrode surface, electrode edges, electrode material, field enhancement at dielectric interfaces, surface flashover, humidity, surrounding atmosphere, temperature, pressure, and excitation time), which are discussed in Chapter 3.

To obtain meaningful critical field strengths, it is necessary to suppress surface flashover around the insulator sides and failure at the electrode edges. Both incidents occur at values below the test materials actual strength. Previous studies either allowed the breakdown at the electrode edge or potted the assembly in silicone rubber to suppress the effects.[7,8,9,10] However, concern has been given to how these silicone rubber encapsulants might contaminate the specimen and, therefore, modify the results. For this reason, a new test cell was developed to study pressed explosive wafers. The design does not allow uncured encapsulants near the test region (between the electrodes). Details of the test cell are described in Chapter 3.

# CHAPTER 2

## DIELECTRIC BREAKDOWN MECHANISMS

To develop possible scenarios for breakdown in explosives, it is helpful to understand the various mechanisms that lead to breakdown in inert insulators. This report does not try to formulate any new breakdown theories for explosives. It is intended to offer possible avenues of thought and to acquaint the reader with the terminology used in dielectric breakdown work.

Dielectric breakdown occurs when the electric field across an insulator reaches a value that allows an electrical arc to pass through it. Before this can occur, a conduction path must be formed under the action of the applied electric stress. It is believed that this conduction path is a filamental channel of ionized gas.[11,12]

### PASCHEN'S LAW

It is tempting to believe that Paschen's Law will predict dielectric breakdown for all insulating materials. Paschen's Law is based on collisional ionization of molecules accelerated by the electric field. Therefore, the breakdown voltage is directly related to the number of ionizable particles between the electrodes. This is demonstrated in Figure 2-1. The breakdown voltage, $V_{BD}$, is plotted against the product of pressure, P, and the electrode spacing, d. Paschen's Law predicts a high breakdown voltage in vacuum, on the far left of the curve, because there are no particles available between the gap for collisional ionization. Holding the electrode spacing constant, the breakdown voltage decreases with increasing pressure to the Paschen minimum as more ionizable particles are introduced in the gap. As the pressure increases past the Paschen minimum, the collision mean free path decreases making it necessary for higher voltages to induce breakdown.

Paschen's Law ultimately fails at very high vacuums and very high pressures due to electron injection from the cathode at high electric field stresses.[13,14] In condensed solids other mechanisms are required to explain dielectric breakdown. However, Paschen's Law cannot be completely forgotten. The partial discharge mechanism discussed below is governed by gaseous discharges bridging tiny air voids existing in the solid. These discharges are dependent on Paschen's Law, therefore, Paschen's Law can dominate breakdown in solid insulators.

### INERT INSULATORS (HOMOGENEOUS SOLIDS)

There are four pathways that lead to dielectric breakdown in solid insulators: the partial discharge mechanism, the electron injection mechanism, the thermal mechanism, and the intrinsic mechanism. Since all four may occur simultaneously, it can be difficult to tell which is dominant.[15] To complicate matters further, it is possible that these four mechanisms are dependent on each other.

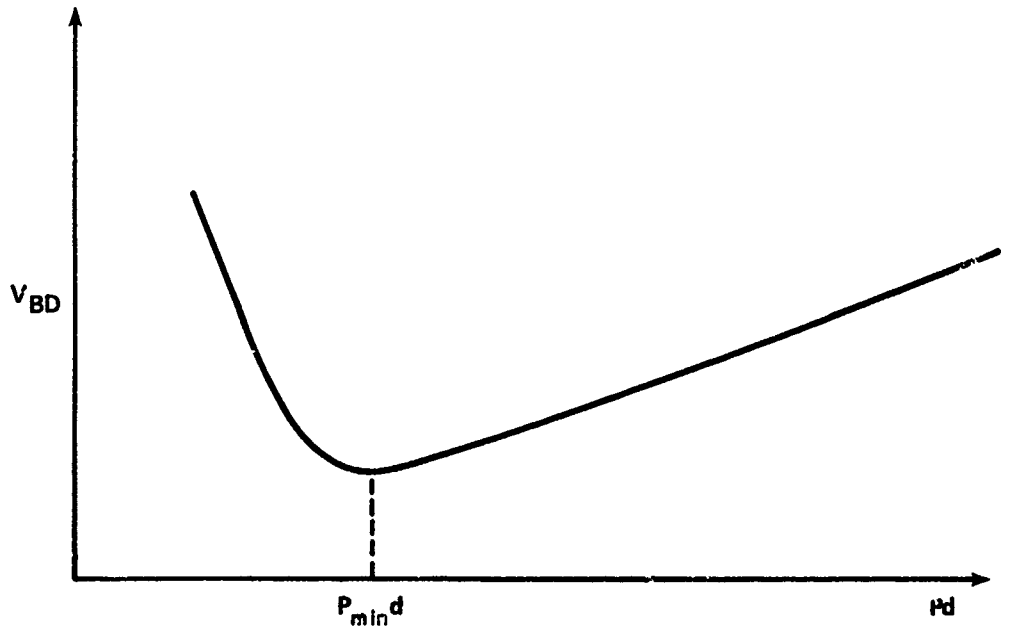


FIGURE 2-1. PASCHEN'S CURVE FOR BREAKDOWN VOLTAGE, $V_{BD}$, VERSUS PRODUCT OF PRESSURE, P, AND ELECTRODE SPACING, d

The Partial Discharge Mechanism is the mechanism of gaseous breakdown in tiny channels of the insulator. It is dominant when small cavities exist in the material which have different dielectric strengths than their surroundings. These cavities can be modeled by a network of capacitances and resistances representing the gases in the cavities and the surrounding solid. A single cavity model is illustrated in Figure 2-2.[16,17]

A fraction of the applied voltage appears across the void as a result of capacitive division. The void capacitance is relatively small because its dielectric constant is close to unity, hence a large voltage stress is applied to the void. As the applied voltage is increased, the field strength across the cavity will reach the critical value of the trapped gas and it will fail. The breakdown current will be limited by the impedance of the surrounding medium, hence the gas recovers and conduction stops. The process repeats itself over and over again; when the conduction stops the electric field recovers and the partial discharge activity recommences. These discharges deform the cavity walls creating tiny capillaries around the periphery of the cavity.[18] The capillaries grow as the partial discharges continue and tree like structures are formed, the trees eventually bridge the electrode gap and allow failure to occur as a result. This is the mechanism of gaseous breakdown in the gas channels.

The Electron Injection Mechanism entails electrons being field emitted from the cathode (Fowler-Nordhein tunneling) and interacting with the insulator's chemical bonds to cause breakdown.[11-14,19-22] How this interaction causes the breakdown is still an open subject.[12] Theorists do agree that whatever the mechanism is, it decomposes the insulator creating voids. Partial discharge activity begins forming trees and breakdown occurs as described above.[11,12,19-22]

Thermal Breakdown occurs as a result of dielectric and conductive losses generating heat.[15,23] There are two processes associated with thermal breakdown: thermal assisted emission of electrons from the cathode and insulator decomposition from direct heating. The only difference between the two is that carrier multiplication arises from thermal emission rather than field emission.[22] The latter occurs when thermal instability is reached in narrow areas causing insulator decomposition.[15,23] This results in void formation and subsequent failure by partial discharge activity.

The Intrinsic Mechanism takes place when the electric field produces interactions between the chemical bonds of the insulator materials to initiate dielectric failure. This particular mechanism is not usually considered because it predicts field strengths larger than what is experimentally measured. Electron injection mechanisms will dominate the breakdown in the presence of electrodes.

## EXPLOSIVES (HETEROGENEOUS SOLIDS)

Dielectric breakdown in explosives has not been extensively studied like other insulating materials. Therefore, the results have been compared to those for inert insulators. Intrinsic and thermal breakdown theories for reactive media have been modeled after those for non-reactive media.[4,5] Tucker et al presented a partial discharge model to explain breakdown in explosive powder-filled spark gaps at 50% density.[6]

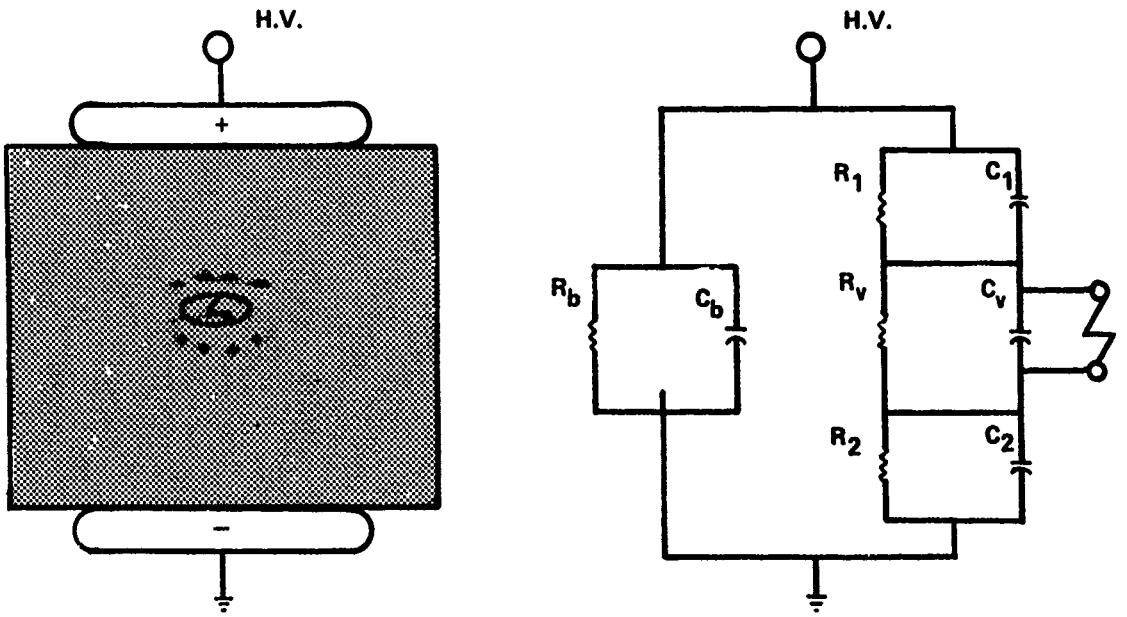


SINGLE VOID IN INSULATOR

SINGLE VOID MODEL

FIGURE 2-2. PARTIAL DISCHARGE MODEL FOR DIELECTRIC BREAKDOWN

The partial discharge model may still be a viable mechanism for condensed plastic bonded explosives. These materials are not manufactured to their theoretical maximum density (TMD). Therefore, voids will exist in the solid allowing partial discharges to occur. Furthermore, these explosives are heterogeneous, unlike most inert insulators, containing explosive crystals and a plastic binder system. It is presumed that the various constituents of the composite explosive have different dielectric constants accompanied by different dielectric strengths. Therefore, the dielectric mismatch between the various constituents may give rise to partial discharges similar to the scenario described above.

# CHAPTER 3

## PROBLEMS IN DIELECTRIC BREAKDOWN MEASUREMENT

Dielectric breakdown appears to be an easy measurement at first, however, the experimentalist will discover very soon that measuring dielectric strength is very difficult. There are many parameters that can dominate the prebreakdown mechanisms and hence, affect the final measurement. If these parameters are not accounted for, the experimentalist will be measuring the performance of his particular test arrangement instead of the dielectric strength of the material in question.

This chapter discusses briefly many of the problems that can affect dielectric breakdown measurements. These include:

1. Electrode Surface
2. Electrode Edges
3. Electrode Material
4. Triple Junction (dielectric boundary adjacent to electrodes)
5. Surface Flashover
6. Humidity
7. Surrounding Atmosphere
8. Temperature
9. Pressure
10. Excitation Time

The adopted solutions are addressed in the following chapter.

ELECTRODE SURFACE - A uniform electrode surface is important for repeatable experiments. High electric field strengths exist at sharp corners such as along scratches and other asperities on the electrode surface. These fields can cause electron emission from the cathode and subsequent dielectric failure described in Chapter 2. Therefore, different results can be obtained from different electrode surfaces.

ELECTRODE EDGES - Similarly, high electric fields will exist at sharp electrode edges even at comparatively low applied voltages. These fields can cause electron emission and external partial discharge activity (corona), which will cause a decrease in the dielectric performance. It is customary to round the electrode edges to decrease the electric field in this region.

ELECTRODE MATERIAL - The work function (energy to free an electron) differs for various electrode materials. This alters the electric field strength required to stimulate field emission from the cathode. Therefore, breakdown via electron injection is affected when different electrode materials are used.

TRIPLE JUNCTION - The electric field at the electrode-air-insulator triple junction, shown in Figure 3-1, can be enhanced as a result of the dielectric mismatch between the air and the insulator material. This phenomenon, discussed in more detail in Appendix A, can increase the local field by a factor close to the ratio of the relative dielectric constants of the two materials. Since the dielectric constant of air is unity and between 2.5 to 5 for high explosives,[6] the electric field can be enhanced by a factor of 2.5 to 5.0.

Higher than average fields around the electrode edges can cause partial discharge activity to occur before normal inception voltages. This external partial discharge activity, called corona, can have the same effect as cavities inside the insulator.

SURFACE FLASHOVER - Another crucial problem is the threat of surface flashover. An insulator will fail along its surface at a voltage well below its bulk breakdown level, unless special care is taken to prevent this.

Problems with triple junction (previously described) and surface flashover are customarily eliminated by either:

1. casting the test material around the electrodes,
2. submerging the test in transformer oil, or
3. potting the test in some other dielectric.

However, excluding PBXW-108(I), the explosives studied were not castable. The pressed explosives (PBX-9404-03, PBX-9501, and PBX-9502) contain many voids as a result of their manufacture, therefore, there was concern that dielectric encapsulants would soak into the test samples and modify the results. So, no uncured encapsulants were allowed near the test region between the electrodes. The test cell and electrodes were designed to overcome these problems.

HUMIDITY, ATMOSPHERE, TEMPERATURE, AND PRESSURE - The effects of humidity, surrounding atmosphere, temperature, and pressure can be understood by considering the partial discharge model. Dielectric breakdown can stem from the onset of partial discharges bridging tiny voids that exist in the materials described in Chapter 2. Therefore, the hold-off voltage of whatever gas is trapped in the voids affects the dielectric strength of the insulator. The hold-off voltage of a gas depends on the above-mentioned items, and affects the bulk properties of the insulator.

EXCITATION TIME - Breakdown processes at a given voltage take time to destroy an insulator. Therefore, excitation time can effect the dielectric strength. It is expected that shorter excitation times will yield larger dielectric strengths. To make meaningful measurements, the excitation time must remain constant.

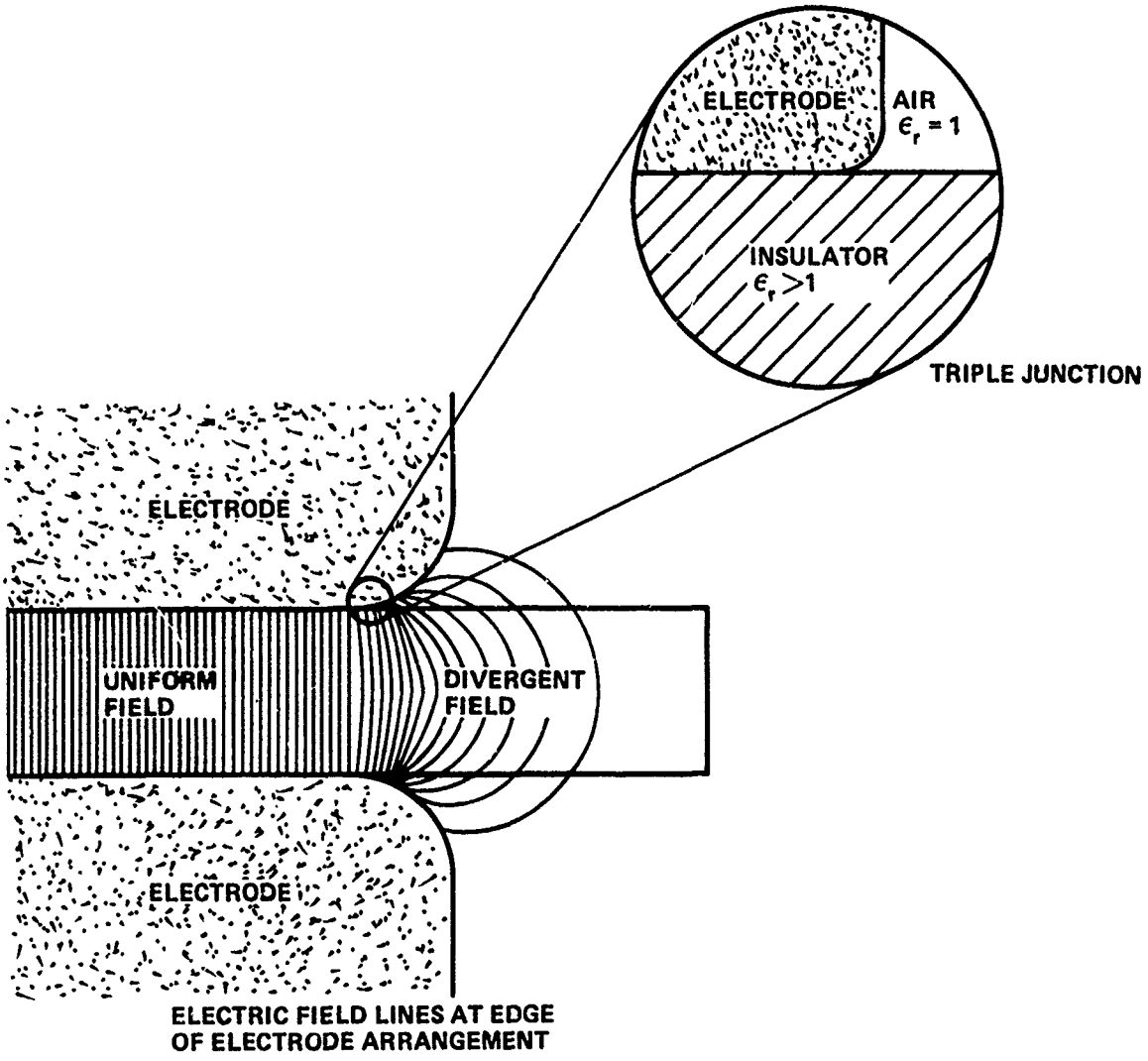


FIGURE 3-1. DIVERGING FIELD AT ELECTRODE EDGE AND TRIPLE JUNCTION

# CHAPTER 4

# EXPERIMENTAL

In previous dielectric breakdown studies, the explosive disc/electrode arrangement was potted in silicone rubber to suppress surface flashover.[7] However, some concern has arisen that these silicone rubber encapsulants might contaminate the specimens and modify the results. For this reason, a new test cell was developed to study pressed explosive wafers. In this cell, uncured encapsulants were not present near the test region.

The test cell and electrodes were designed to control:

1. the electrode surface (by polishing);
2. field concentration at electrode edges (by rounding edges);
3. field enhancement at the electrode, air, insulator triple junction (by a shielding technique at electrode edges); and
4. surface flashover (by test cell construction).

The experimental procedure was designed to control:

1. humidity (by keeping samples in a dessicator prior to testing), and
2. excitation time (by manually increasing voltage 1 kV every 5 seconds until failure).

The following section discusses in more detail how the parameters were dealt with for this study. This chapter also contains a section on how the various explosives were manufactured for this study.

## ELECTRODES

Explosive samples were tested between brass electrodes forming a plane to plane configuration to obtain a well defined, uniform field. The electrodes were 19 mm (3/4") diameter, 7.5 mm (3/8") long cylinders. A 3.2 mm (1/8") radius at the edges was employed to decrease the divergent field in that region. Tests showing dielectric failures at the electrode edges would be considered invalid since the divergent field at the electrode edges is ill-defined. Therefore, care was taken to insure failure occurred in the uniform field region towards the center of the electrodes.

Electrodes were polished before each test to remove asperities caused by previous tests. The polishing procedure consisted of removing electrical arc damage with a 600 grit silicon carbide sandpaper, then polishing to a mirror finish with "jeweler's rouge." The electrode surfaces were cleaned by a soap and water solution and finally degreased with methanol.

To eliminate the triple junction effect, a polyurethane base epoxy EN7 by Conap[24] was cast around the cathode electrode (shown in Figure 4-1). The epoxy used had a relative dielectric constant ($\varepsilon_r \approx 3.0$) similar to that of

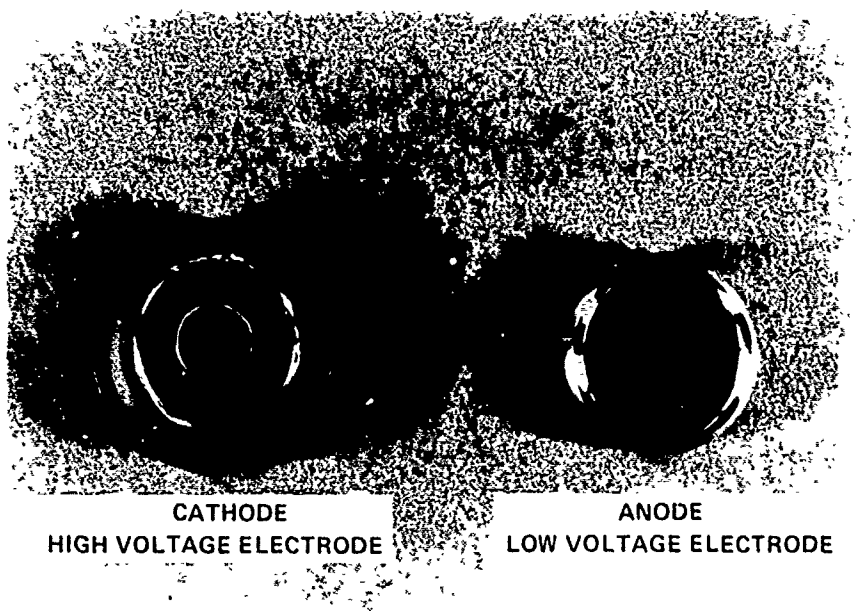


**FIGURE 4-1. PHOTOGRAPH OF FINISHED ELECTRODES**

the high explosive sample so the dielectric mismatch was reduced. After preparing the electrode surfaces, a thin film [0.010" (0.25 mm) thick] of silicone rubber RTV 615[25] was applied at the cathode edge overlapping the electrode and the epoxy surfaces. The RTV 615[25] was allowed to cure for 24 hours. A dielectric cover was placed over the electrode edge area, thus insuring dielectric failure would occur towards the center of the electrode. Only the cathode received this special treatment since it is the offending electrode, where electrons are emitted. In this case, the cathode is the high voltage electrode where corona may occur.

TEST CELL

The test cell was designed to contain the electrode and suppress surface flashover, inside and outside the cell. The following subsections describe how the test cell was constructed and modified to accommodate the various explosives tested.

Pressed High Explosives - A photograph of the test cell employed is shown in Figure 4-2. A convoluted path of PMMA was provided inside and outside the test cell between the high voltage electrode and ground to suppress surface flashover. The pressed explosives PBX-9404-03, PBX-9501, and PBX-9502 were fabricated into 38.1 mm (1.5") diameter discs. These explosive discs and the electrodes, previously discussed, were mounted in the test cell as indicated in Figure 4-3.

The anode was spring loaded from the base plate in an attempt to compress the RTV gasket shielding the cathode triple junction, so that the sample would make contact with both electrodes. However, it is believed that the sample did not make good contact with the cathode. This method is compared to a similar technique where proper contact was achieved between cathode and sample in Chapter 5. It is shown that the data from both techniques are comparable. The sample thickness set the electrode spacing. Surface flashover around the sample was suppressed by applying silicone rubber encapsulant RTV 3145[26] around the sample's periphery, thereby glueing the sample to the inside ledge of the test cell. This procedure eliminated the possibility of encapsulant contaminating the test region between the electrodes.

Cast High Explosives - PBXW-108(I) was cast in a similar test cell shown in Figure 4-4. The grounded anode was threaded from the bottom of the test cell so the gap could be set prior to casting. The epoxy[24] and RTV[25] around the cathode was not required for these tests, since both electrodes were cast inside the explosive eliminating the possibility of a triple junction.

Detasheet Type C - Dupont's Detasheet Type C[1] was tested using the same cathode configuration shown in Figure 4-3. These sheets are naturally soft, therefore, the anode was not spring loaded, otherwise, the anode would penetrate the soft explosive. The anode was gently pushed into place against the "Detasheet" and held there by a retaining screw.

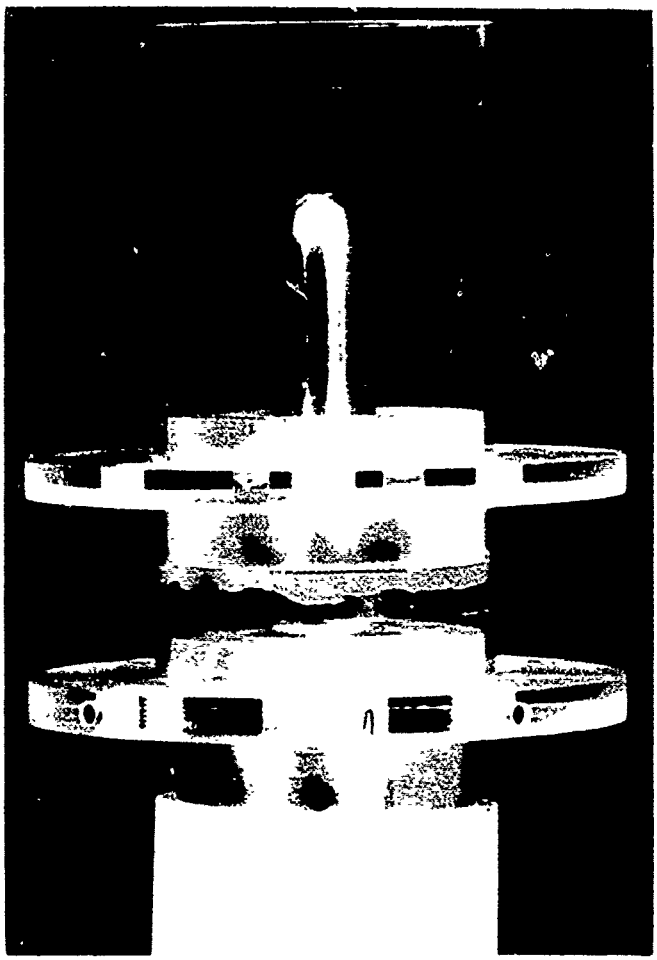

FIGURE 4-2. PHOTOGRAPH OF STATIC DIELECTRIC BREAKDOWN TEST CELL

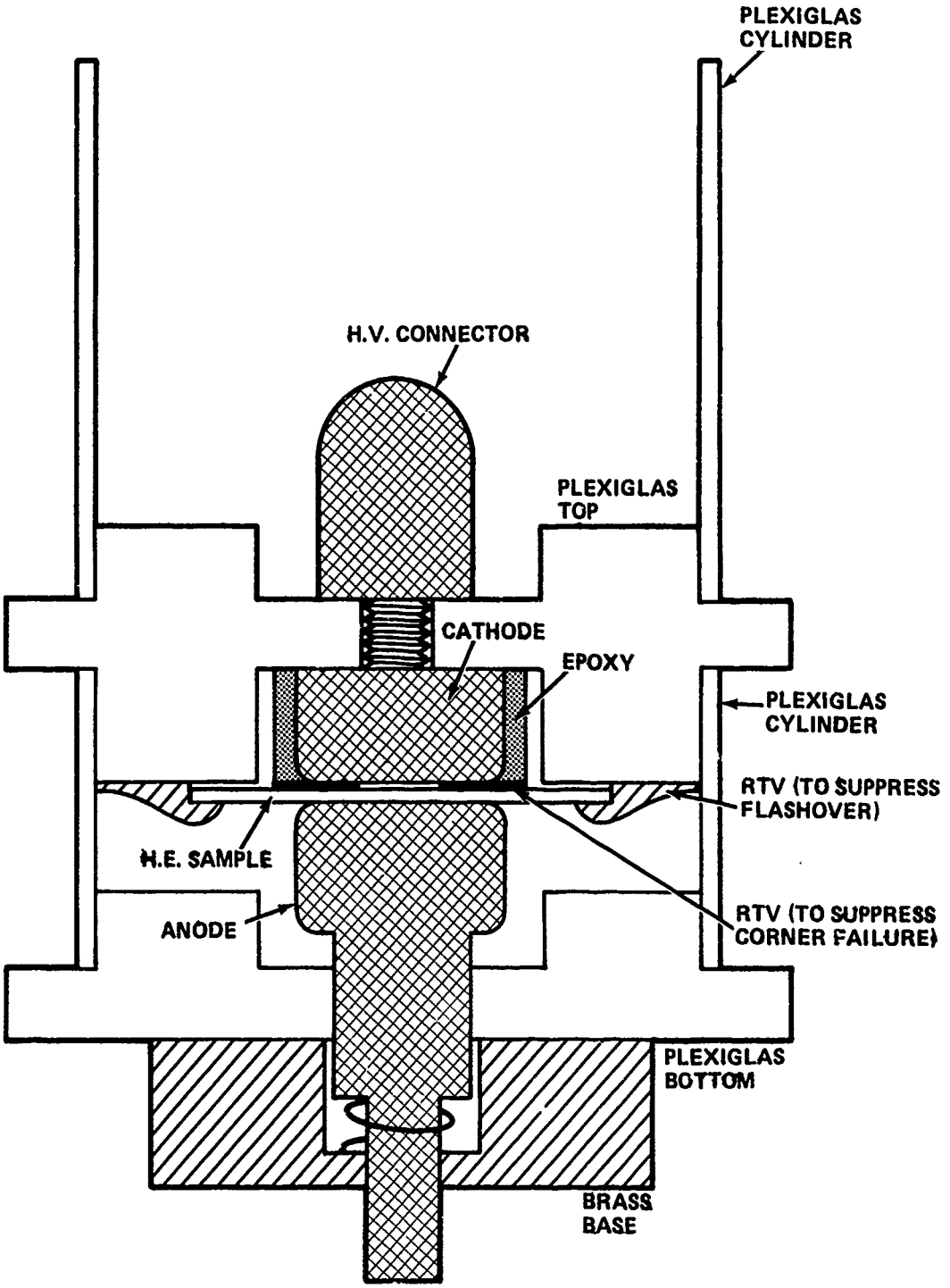


FIGURE 4-3. STATIC DIELECTRIC BREAKDOWN TEST CELL FOR PRESSED HIGH EXPLOSIVES

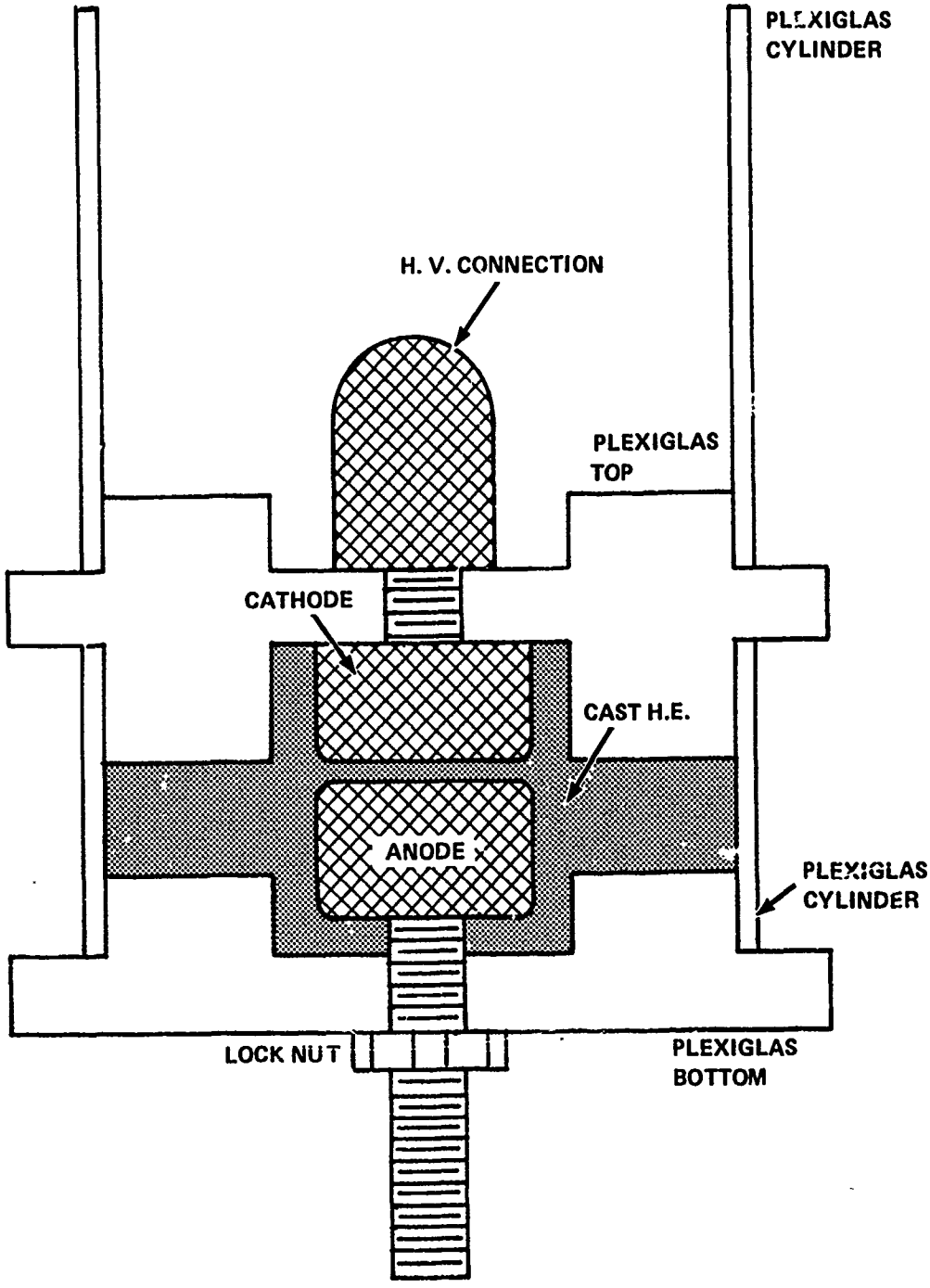


FIGURE 4-4. STATIC DIELECTRIC BREAKDOWN TEST CELL FOR CAST HIGH EXPLOSIVES

## EXPLOSIVES

Explosives are heterogeneous materials comprised largely of an energetic material like HMX, RDX, TATB or PETN, and an inert binder system. Table 4-1 contains information about the formulations and densities for the explosives tested.[1, 26, 27]

Pressed High Explosives - PBX-9404-03, PBX-9501, and PBX-9502 shared a similarity in morphology in that they were originally pressed from elliptical agglomerates. These agglomerates are shown on the left side in Figure 4-5. The explosive crystals are combined with the binder in a slurry. The agglomerates are formed from this mixing. The agglomerates in turn are placed in an isostatic press to form the solid explosive.

The PBX-9404-03 was pressed at the Naval Surface Weapons Center, White Oak. The explosive was pressed inside a rubber boot with a mild vacuum applied inside the boot and was heated to 100°C. The explosive's pressing density is obtained after three consecutive pressings. The first pressing is performed at 10,000 psi for 10 minutes, the second at 20,000 psi for 10 minutes, and the third at 30,000 psi for 15 minutes.

After pressing the solid block of PBX-9404-03, the explosive was allowed to cool at ambient temperature. The explosive was then machined on a lathe into the wafers used for the tests. One such wafer is shown in Figure 4-5.

The PBX-9501 and PBX-9502 explosives were pressed similarly at Los Alamos National Laboratories. The fabrication of the PBX-9501 and PBX-9502 wafers was performed at the Naval Surface Weapons Center, White Oak.

Cast High Explosives - The PBXW-108(I) is an RDX base material with a polyurethane binder that is cured at room temperature. The PBXW-108(I) constituents were mixed in a Baker Perkin's High Shear Vertical Mixer. The binder system is mixed at 15 minute intervals, adding an ingredient at a time. The RDX was added last and mixed with the binder for 15 minutes. The mixture was then poured into the test cell under vacuum. The test cell was vibrated to make sure the explosive settled properly. After casting, the explosive was stored at ambient temperature overnight. X-ray photographs were taken of the PBXW-108(I) in the test cell to ensure no air bubbles were present between the electrode gaps.

Detasheet Type C - The details concerning the manufacture of DuPont's Detasheet Type C[1], are proprietary. The explosive is extruded into presses where the final shape is formed. The Detasheet Type C[1] was cut into wafers from a 1 mm sheet of the material.

## TEST PROCEDURE

The test cells were placed inside a confinement tank, capable of containing the fragments and explosive gases in case of initiation. The test was viewed and recorded remotely via a closed circuit television system. Figure 4-6 shows a schematic of the test circuit. A direct voltage was applied across the test sample by a Hipotronics 120 kV D.C. variable power supply. The voltage was manually increased 1 kV every 5 sec via a variac

TABLE 4-1. NAMES AND FORMULATIONS OF HIGH EXPLOSIVES

| Explosive | Formulation Ingredient | Wt.% | Density, $\rho$(g/cm$^3$) TMD | Nominal | Color |
|---|---|---|---|---|---|
| PBX-9404-03[27] | HMX | 94 | 1.865 | 1.83-1.84 | blue |
| | NC[a] (12.0%N) | 3 | | | |
| | CEF[b] | 3 | | | |
| PBX-9501[27] | HMX | 95 | 1.855 | 1.84 | white |
| | Estane[c] | 2.5 | | | |
| | BDNPA-F[d] | 2.5 | | | |
| PBX-9502[27] | TATB | 95 | 1.942 | 1.90 | yellow |
| | Kel-F-800[e] | 5 | | | |
| PBXW-108(I)[28] | RDX Class D[f] | 52.6 | NA | 1.56 | white |
| | RDX Class C[g] | 10.2 | | | |
| | RDX Class A[h] | 6.9 | | | |
| | RDX Class E[i] | 15.3 | | | |
| | R45HT[j] | 7.0 | | | |
| | DOA[k] | 7.0 | | | |
| | Cyanox 2246[l] | 0.1 | | | |
| | PAPI[m] | 0.9 | | | |
| Detasheet Type C[1] | PETN | 64.5 | - | 1.48 | olive |
| | NC[a] (12.3%N) | 8 | | | |
| | ATBC[n] | 27.5 | | | |

[a]NC - Nitrocellulose
[b]CEF-Tris-β - chloroethylphosphate
[c]Estane - Polyurethane solution system
[d]BDNPA-F - Bis(2,2-dinitropropyl)Acetal/bis(2,2-dinitropropyl)Formal, 50/50 wt %
[e]Kel-F-800 - Chlorotrifluoroethylene/Vinylidine Fluoride Copolymer, 3:1
[f]RDX Class D - 100% US standard seive USSS no. 8 (i.e. 2380 m) and 20±20% USSS no. 35 (i.e. 500 m)
[g]RDX Class C - 99% USSS no. 12 (i.e. 1680 m), 40±10% USSS no. 50 (i.e. 297 m) 20±10% USSS no. 100 (i.e. 149 m), and 10±10% USSS no. 200 (i.e. 74 m)
[h]RDX Class A - 98±2% USSS no. 20 (i.e. 840 m), 90±10% USSS no. 50 (i.e. 297 m), 60±30% USSS no. 100 (i.e. 149 m), and 25±20% USSS no. 200 (i.e. 74 m)
[i]RDX Class E - 97% USSS no. 325 (i.e. 44 m)
[j]R45HT - Polybutadiene, linear
[k]DOA - Di(2-ethylhexyl)adipate
[l]Cyanox 2246 - An antioxidant
[m]PAPI - Polymethylene Polyphenylisocyanate
[n]ATBC - Acetyltributylcitrate

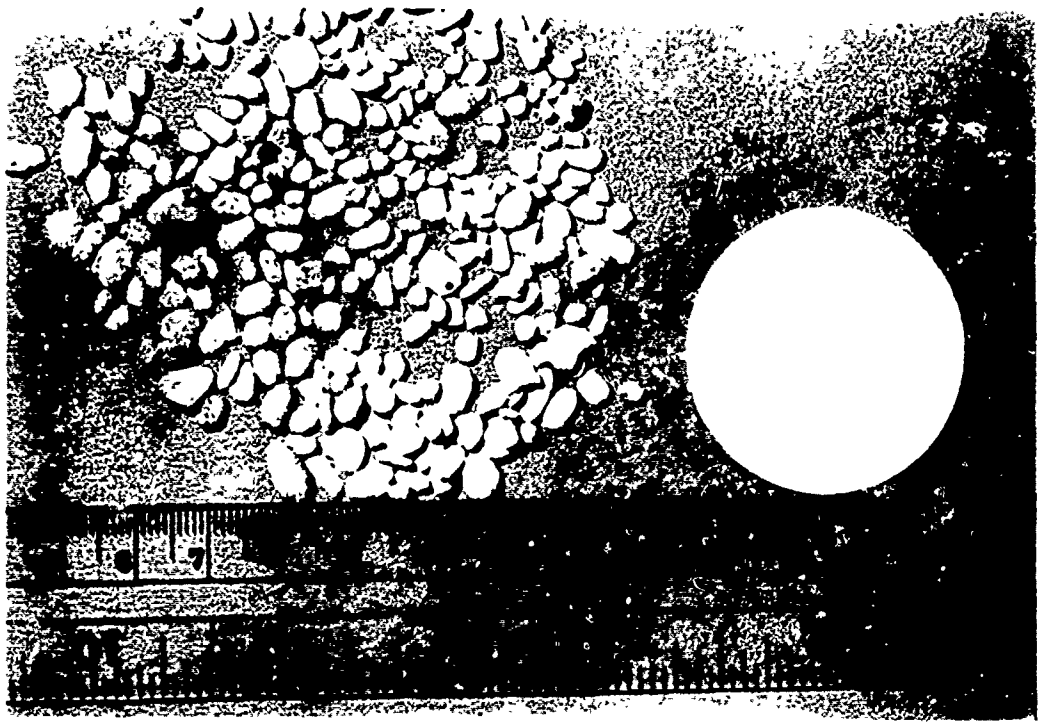

FIGURE 4-5. PHOTOGRAPH OF PBX-9404-03 BEFORE AND AFTER PRESSING OF AGGLOMERATES

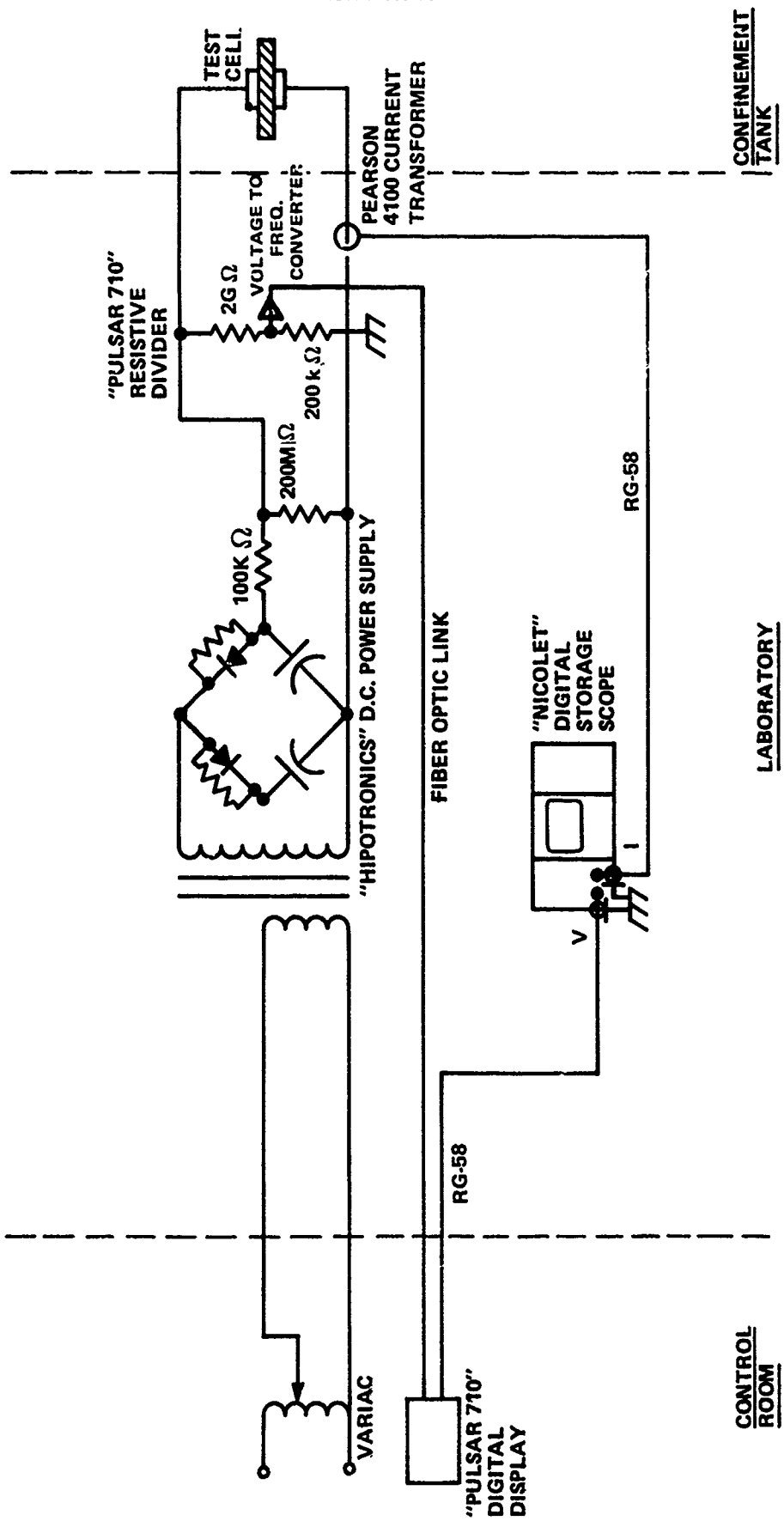


FIGURE 4-6. SCHEMATIC OF TEST CIRCUIT

control unit provided with the power supply. The voltage was measured by a Pulsar 710 fiber-optically isolated resistive divider and recorded on a Nicolet digital storage oscilloscope.

A Nicolet digital oscilloscope was used to monitor the voltage and current. When breakdown occurred, current in the ground return, detected by a Pearson 4100 (1 volt/amp) current transformer, triggered the oscilloscope. The oscilloscope thus recorded the voltage level immediately prior to dielectric failure of the sample.

# CHAPTER 5

# RESULTS

Results from dielectric breakdown studies on five explosives are given in Table 5-1. Mean critical field strengths, $E_c$; sample thickness; density; percent void concentration; and the number of tests on each explosive are given. Results from previous work on PBX-9404-03 and PBXW-108(I) are presented in parentheses just under the present results.

## PBX-9404-03 (PRESSED FROM AGGLOMERATES)

Results for PBX-9404-03, an HMX material pressed from agglomerates, are shown for 1 mm and 1.5 mm thick samples. The 1 mm thick samples demonstrated an $E_c$ of 13.1 kV/mm substantially lower than previously reported (18.97 kV/mm).[7] Furthermore, the standard error of the results was quite high (± 2.8 kV/mm). The standard error was brought to a respectable level (± 0.6 kV/mm) by increasing the sample thickness to 1.5 mm. However, $E_c$ remained comparably low (14.6 kV/mm).

## PBX-9404-03 (PRESSED FROM POWDER)

PBX-9404-03, from the same batch as the above samples, was machined into a powder and repressed to determine if the change in morphology would affect $E_c$. The 1 mm thick samples of PBX-9404-03 pressed from powder displayed a strength of 29 kV/mm, a 120% increase in $E_c$ over that for PBX-9404-03 pressed from agglomerates (13.1 kV/mm).

## PBX-9501

Results for PBX-9501, another HMX-based material pressed from agglomerates, display an $E_c$ comparable to that for PBX-9404-03 pressed from agglomerates.

## PBX-9502

PBX-9502, a TATB-based material with a KeL-F binder, had a surprisingly high critical field strength (40 kV/mm); the possible reasons for this are discussed in Chapter 6.

## PBXW-108(I)

Dielectric breakdown was tested for PBXW-108(I) over a range of thicknesses, 1 to 5 mm. This data, plotted in Figure 5-1, does not demonstrate any significant correlation between $E_c$ and material thickness over the thicknesses tested. Therefore, the result displayed in Table 2 was obtained by taking a best fit to the data.

TABLE 5-1. CRITICAL FIELD STRENGTHS FOR HIGH EXPLOSIVES

| Explosive | Main Ingredient | Sample Thickness d (mm) | Mean Density $\tau_o$ (g/cm$^3$) | Percent Void Concentration | Mean Critical Field Strength[a] $E_c$ (kV/mm) | No. of Charges Tested |
|---|---|---|---|---|---|---|
| PBX-9404-03 (Agglomerates) | HMX | 1 | 1.816 ± 0.003 | 2.63 | 13.1 ± 2.8 | 7 |
| PBX-9404-03 (Agglomerates) | HMX | 1.5 | 1.839 ± 0.012 | 1.39 | 14.6 ± 0.6 (18.97)[b] | 5 |
| PBX-9404-03 (Powder) | HMX | 1 | 1.78 ± 0.015 | 4.56 | 29.0 ± 1.8 | 5 |
| PBX-9501 (Agglomerates) | HMX | 1 | 1.783 ± 0.001 | 3.9 | 14.3 ± 2.4 | 4 |
| PBX-9502 (Agglomerates) | TATB | 1 | 1.903 ± 0.006 | 2.0 | 40.0 ± 2.7 | 5 |
| PBXW-108(I) (Cold Cast) | RDX | 1 to 5 | 1.56 ± 0.005 | 1.0 | 21.7 ± 3.1 (18.42)[b] | 9 |
| Detasheet Type C[c] | PETN | 1 | 1.48 | --- | 16.1 ± 0.6 | 7 |

[a]The error is the standard error of the mean = $\sqrt{\frac{\text{sample variance}}{(n-1)}}$, where n is the number of charges tested.

[b]Reference 7

[c]Sample of Detasheet Type C[1] at edge of electrodes, therefore, the actual value is larger than that indicated.

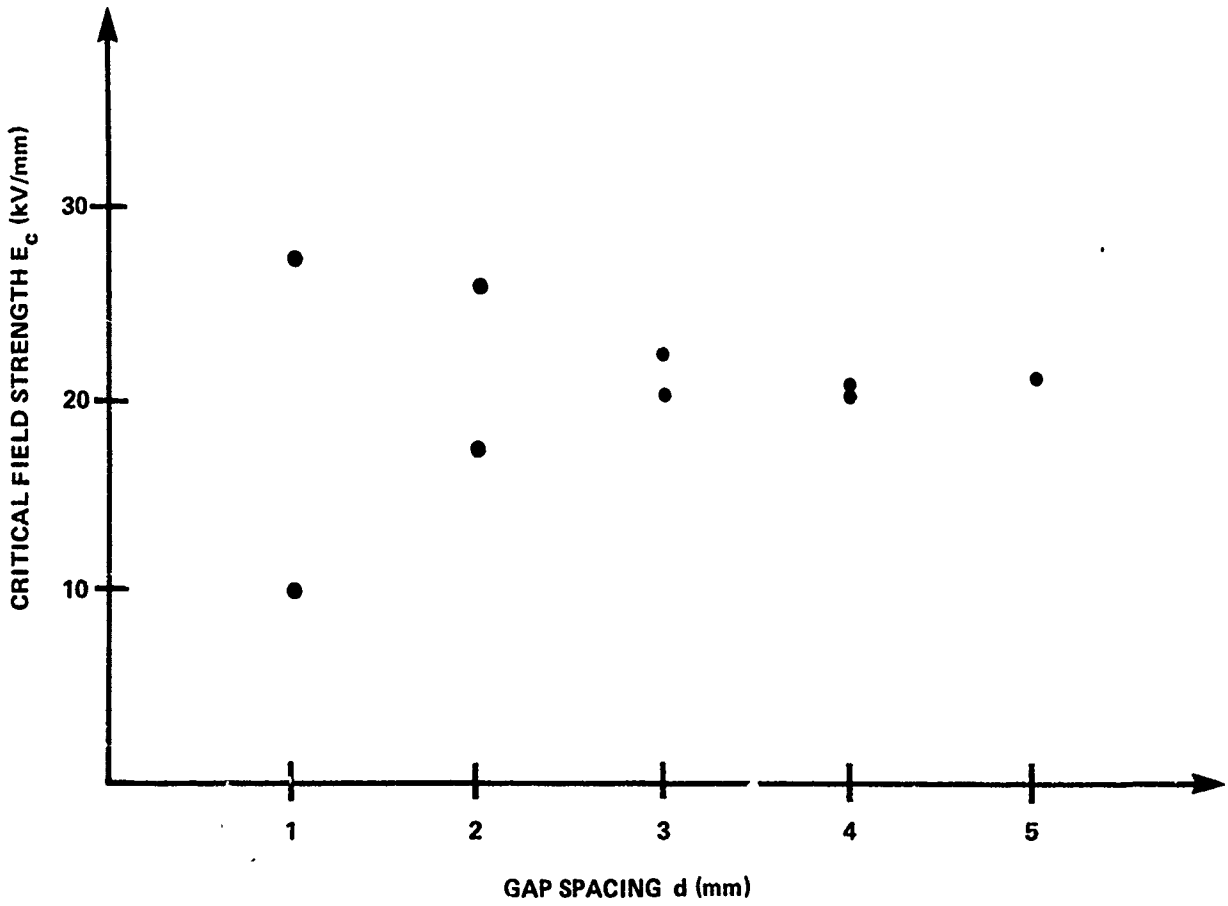


FIGURE 5-1. CRITICAL FIELD STRENGTH, $E_c$, vs GAP SPACING, d, FOR PBXW-108(I)

DETASHEET TYPE C

The dielectric breakdown data for Detasheet Type C[1] should be considered the lower bound of the actual $E_c$. The material is so soft that the slightest pressure from the electrodes caused necking at the edges. Therefore, failure occurred in a thin region at the electrode edge despite the RTV 615 gasket.

VERIFICATION OF RESULTS

To suppress failure at the electrode edges, a silicone rubber (RTV 615)[25] covered the cathode triple junction. No matter how much the RTV gasket compressed under the force of the spring-loaded anode, it is presumed the specimen did not make complete contact with the cathode. Therefore, a tiny void existed between the cathode and the sample where partial discharge activity may have occurred. Most failures were located at the edge of the gasket between the electrodes. This was verified by observations of the arc damage to the electrodes shown in Figure 5-2 which indicates that the gasket did have an effect on breakdown.

An improved method for shielding the triple junction has been developed since the above tests were performed. The epoxy cast around the cathode was changed to Epon 815 (Epon 815 Resin,[29] Ancamine T-1 hardener[30]). A thin layer of the epoxy was allowed to cover the cathode surface. This insulates the triple junction at the edges, thus eliminating the need for the RTV gasket. The central region is cleaned away to allow contact with the explosive. An oversized (15/16" diameter) anode was used to help reduce the field at the cathode edges.

Explosive samples were tested under identical conditions using both techniques. The results are shown in Table 5-2. These results agree within the standard error of the RTV gasket technique. Therefore, the results reported in Table 5-1 are a good indication of dielectric breakdown strengths for the five explosives studied. The epoxy cast cathode technique (new method) has an improved standard error which indicates this technique is preferable over the other.

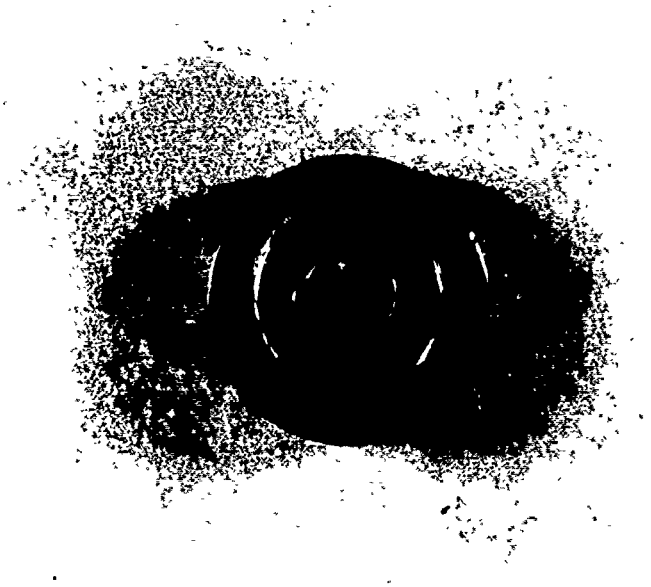

FIGURE 5-2. PHOTOGRAPH OF ARC DAMAGED HIGH VOLTAGE ELECTRODE

TABLE 5-2. CORRELATION BETWEEN TRIPLE JUNCTION SHIELDING TECHNIQUES

| Technique | Mean Critical Field Strength ($E_c$) | Standard Deviation | Standard Error | Number Tested |
|---|---|---|---|---|
| Epoxy Cast[a] Over Cathode | 21.28 kV/mm | 0.68 | 0.39 | 3 |
| RTV Gaskets[b] Over Cathode | 24.15 kV/mm | 3.24 | 1.62 | 4 |

a. An epoxy, Epon 815 resin,[29] Ancamine T-1 hardner,[30] was cast around the cathode which allowed a thin layer of the epoxy to cover the electrode edge.

b. A thin gasket of silicone rubber RTV 615[25] shielded the cathode edge. An epoxy, EN7 by Conap,[24] was cast around the cathode to provide a base for the RTV gasket to rest on.

# CHAPTER 6

# DISCUSSION

## PBX-9404-03 (PRESSED FROM AGGLOMERATES)

The breakdown values for 1 mm thick PBX-9404-03 varied from 9 kV/mm to 23 kV/mm. The wide scatter for these samples was probably due to the particulate nature of each sample. Samples were pressed from irregular agglomerates with dimensions on the order of 1 mm, like those shown in Figure 4-5. The agglomerate size was thus comparable with the sample thickness allowing interstitial breakdown to result. The interstices between the agglomerates constituted a low density path that bridged the electrode gap which led to a reduction in the breakdown strength. It is possible that the 1.5 mm thick samples suffered from similar effects which would explain the low breakdown level of 14.6 kV/mm compared to previous results of 18.97 kV/mm[7] and 22.2 kV/mm.[8] The variation in these data shows a dependence on morphology and perhaps test method aside from the dependence on the explosive composition.

## PBX-9404-03 (PRESSED FROM POWDER)

Samples of PBX-9404-03 pressed from powder indicate an improvement in $E_c$. Specimens from both pressings are compared in Figure 6-1. It can be seen from Figure 6-1 that the interstitial structure for the pressed powder is much finer than that for the pressed agglomerates Therefore, the interstices did not bridge the gap resulting in an $E_c$ of 29 kv/mm. So, $E_c$ was over 120% larger for pressed powder than for pressed agglomerates (13 kV/mm) despite the 2% reduction in pressing density.

Fine particle size explosives are more difficult to press to high densities than are coarse particle size explosives. The reduction in pressing density would seem to work to decrease $E_c$. However, with sample thicknesses comparable to agglomerate sizes, the interstices governed the breakdown behavior. It is expected that $E_c$ for pressed agglomerates will increase to values close to that for pressed powder as the sample thickness increases.

## PBX-9501

The similarity in $E_c$ for PBX-9501 and PBX-9404-03 is not surprising since they are of similar composition (95% and 94% HMX respectively). However, in light of results discussed above, the similarity in $E_c$ most likely stems from the similarity in morphology. The agglomerate size is similar for both materials prior to pressing. It is expected $E_c$ will improve for PBX-9501 if the agglomerate size is reduced.

## PBX-9502

PBX-9502 has an exceptionally high dielectric strength (40 kV/mm) compared to the results for TATB (5.75 kV/mm),[7] which is the main ingredient

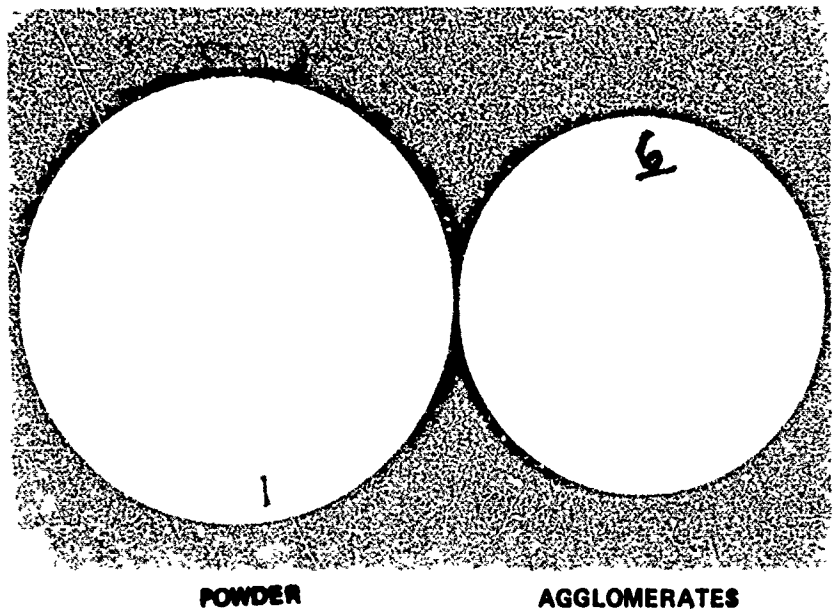


FIGURE 6-1. PHOTOGRAPH OF PBX-9404-03 PRESSED FROM POWDER COMPARED TO PBX-9404-03 PRESSED FROM AGGLOMERATES

for PBX-9502 (95%). It is presumed that the improved breakdown value for PBX-9502 over its main ingredient can be attributed to the Kel-F binder and the consequent improvement in pressing density. It is further presumed that the slightly smaller agglomerate size linked with the higher pressing density for PBX-9502 compared to PBX-9404-03 and PBX-9501 allow for the larger breakdown value.

PBXW-108(I)

The data for PBXW-108(I) displays significant scatter; it is not possible to detect a dependence on gap spacing. Typically, a degradation in critical field strength is experienced in inert insulators as spacing is increased. This is associated with an increase in void concentration. Perhaps larger gap spacings are required to determine any dependence on material thickness.

DETASHEET TYPE C

The Detasheet Type $C^1$ always failed at the electrode edge as a result of the material necking when pinched between the electrodes. Failure at the edges has been associated with reduced critical field strengths. Therefore, these results are given as a lower boundary of dielectric performance for Detasheet Type $C^1$.

INITIATION OF EXPLOSIVES

None of the explosive samples either burned or exploded as a result of these tests. Some evidence of burning was found close to where the arc punctured the sample for several PBX-9404-03 samples. However, for the most part, the samples were merely punctured as a result of the arc passing through it. Figure 6-2 shows typical specimen damage.

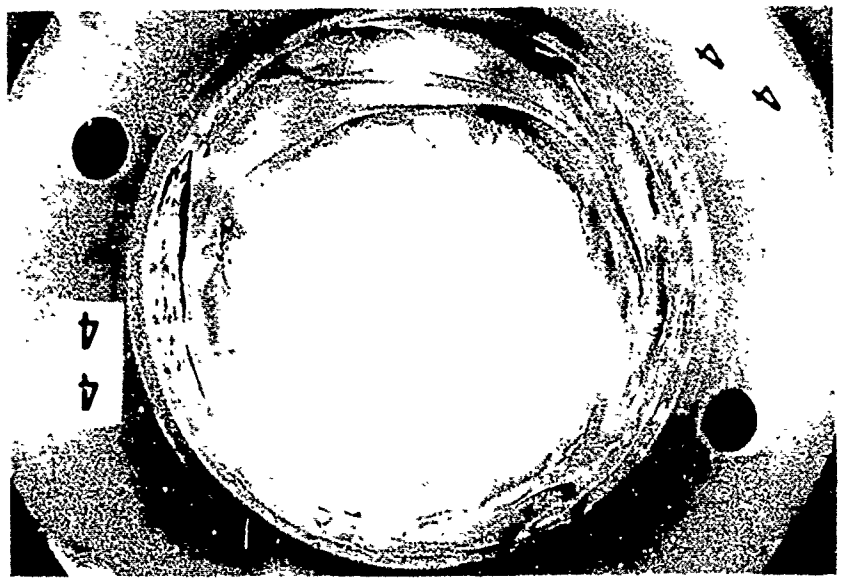

BEFORE DIELECTRIC BREAKDOWN

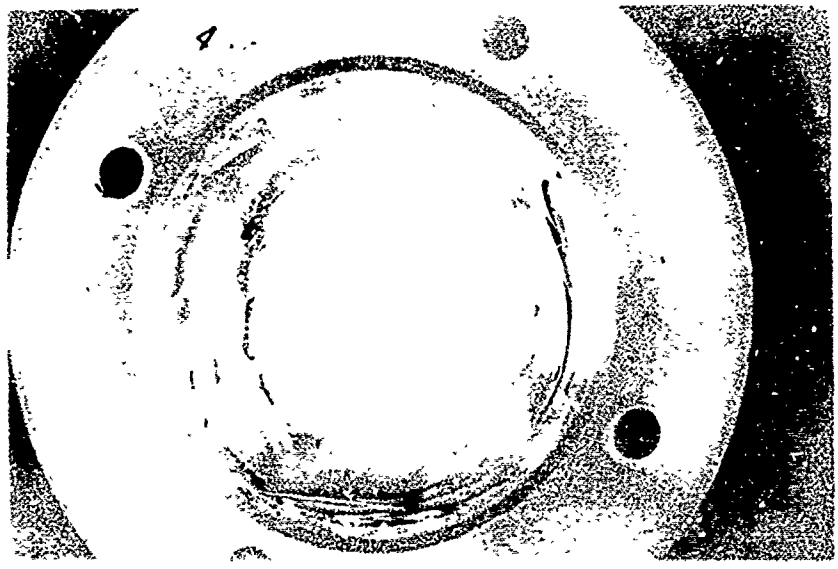

AFTER DIELECTRIC BREAKDOWN

FIGURE 6-2. PHOTOGRAPHS OF PBX-9404-03 BEFORE AND AFTER DIELECTIC BREAKDOWN TEST

# CHAPTER 7

# FUTURE WORK

This report suggests that dielectric breakdown in composite secondary explosives is dominated by partial discharge activity in existing air voids or between constituents of varying dielectric constant. Therefore, partial discharge measurements and studies on the effect of morphology, thickness, humidity, and excitation time are recommended.

## PARTIAL DISCHARGE MEASUREMENTS

It has been stated that the inclusion of voids in plastic bonded explosives may allow partial discharge activity to dominate dielectric breakdown. Studies to measure partial discharges in explosives to correlate their relevance to breakdown are recommended.

Processes leading to breakdown (such as partial discharge activity) occur on a nanosecond time scale. Therefore, inductance existing between the test specimen and the power source can modify these processes and affect the dielectric strength.[31] To eliminate this source of error, the high voltage source must be isolated from the insulator via a large resistance. The energy source can be a capacitance connected through a low inductive transmission line to the electrode geometry. Future work is recommended to study the effect of various capacitances on the dielectric strength.

## MORPHOLOGY STUDIES

It has been established that morphology can dominate the breakdown process in pressed explosives. More definitive measurements are recommended for PBX-9501 and PBX-9502 with different agglomerate sizes.

## SAMPLE THICKNESS

Critical field strength for inert insulators displays a dependence on sample thickness. Tests are recommended to determine similar trends for explosives.

## HUMIDITY DEPENDENCE

Preliminary results, not reported here, indicate that the dielectric strength for PBX-9502 has a strong dependence on humidity. Tests are recommendd to quantify this dependence.

## TIME DEPENDENCE

It is expected that the critical field strength will increase for short duration pulsed excitations. Tests are recommended to substantiate this statement.

INCREASE DATA BASE

The data base should be increased by studying PBXW-113 and some aluminized explosives like PBXW-115, PBXW-103, and PBXW-105.

# CHAPTER 8

# CONCLUSIONS

The critical field strength for PBX-9404-03 (13.1 kV/mm), PBX-9501 (14.33 kV/mm), PBX-9502 (40 kV/mm) PBXW-108(I) (21.7 kV/mm), and Detasheet Type C[1] (16.1 kV/mm) are comparable or greater than that for polyethylene (18 kV/mm).[2] Therefore, these materials can be considered good insulators in their unreacting states.

The results indicate that the critical field strengths of the pressed explosives are strongly influenced by their morphology. The critical field strength can be enhanced by reducing the agglomerate size and increasing the pressing density.

Pressed explosives contain air voids. This is evident from comparing actual pressing densities to theoretical maximum densities (TMD) for these explosives. It is, therefore, easy to imagine that partial discharge activity in these voids dominates dielectric breakdown in pressed explosives. However, more definitive experiments (partial discharge measurements) are required to prove this statement.

The void structure is different for cast PBXW-108(I); however, the critical field strength for PBXW-108(I) is on the same order of magnitude as those for pressed explosives. It is, therefore, speculated that breakdown for PBXW-108(I) is dominated by partial discharge activity in either air voids or regions where the constituents provide a dielectric mismatch.

The breakdown mechanisms were also given to help the reader understand the experimental parameters that can affect the dielectric breakdown. These parameters are: electrode surface, electrode edges, electrode material, field enhancement at triple junction (dielectric mismatch adjacent to electrode), surface flashover, humidity, surrounding atmosphere, temperature, pressure, and excitation time. If these parameters are left unchecked, the experimenter will only measure the dielectric performance of his test arrangement and not the dielectric strength of the material in question.

Thus far, this effort has developed techniques to control the electrode surface, reduce field enhancement effects at the electrode edges (round electrode edges and shield the triple junction), and suppress surface flashover. A silicone rubber (RTV)[26] gasket was used to shield the triple junction for pressed composite wafers instead of encapsulating the test arrangements, like previous studies. PBX-9404-03 is the only pressed composite that can be compared to earlier work. Unfortunately, no conclusion can be made by this comparison in lieu of the morphology effect.

The method used to shield the electrode edges prevented the explosive from making contact with the cathode, allowing an air gap to separate them. This method, however, was favorably compared to an improved technique which

allowed contact between explosives and cathode. The air gap did not affect the results because the air probably failed prior to failure in the solid. Therefore, the entire voltage was applied across the sample.

## REFERENCES


1. "DuPont Detasheet, Flexible Explosive," Type C, E. I. duPont de Nemours & Co. (Inc.), Explosives Products Division, Explosives Specialties Sales, Wilmington, Delaware 19898.

2. Handbook of Chemistry and Physics, Chemical Rubber Publishing Company, 40th Edition, 1958-1959.

3. Tasker, D. G., The Properties of Condensed Explosives for Electromagnetic Energy Coupling, NSWC TR 85-360, Naval Surface Weapons Center, 1985.

4. Frankel, M. J., Theory of Dielectric Breakdown in Reactive Media, NSWC TR 79-331, Naval Surface Weapons Center, Jun 1980.

5. Zakharov, Yu. A., Sukhushin, Yu. N., "An Investigation of Electrical Breakdown and Excitation of Detonation in Thallium and Copper Azides," Izvestiya Tomskogo Ordona Truduvogo Klasnogo Znameni Plitekhnicheskogo Instituta, Vol. 251, Tomsk, 1970.

6. Tucker, T. J.; Kennedy, J. E.; and Allensworth, D. L., Secondary Explosive Spark Detonators, SC-R-713486, Sandia Laboratories, Albuquerque, NM 87115.

7. Demske, D. L.; Forbes, J. W.; and Tasker, D. G., "High Current Electrical Resistance of PBX-9404 and Dielectric Breakdown Measurements of Naval High Explosives," Shock Waves in Condensed Matter, edited by J. R. Asay, R. A. Grahan, and G. K. Straub (North-Holland, Amsterdam, 1983), pp. 551-554.

8. Encyclopedia of Explosives and Related Items, PATR 2700, 5, 1972, p. 1221.

9. Walbrecht, E. E., Dielectric Properties of Some Common High Explosives, Technical Memorandum 1170, Picatinny Arsenal, Apr 1963.

10. Leopold, H. S., Exposure of Primary Explosives to Applied Electric Fields, NOLTR 73-125, Naval Ordnance Laboratory, 1973.

11. Inuishi, Y., "Effect of Space Charge and Structure on Breakdown of Liquid and Solid," IEEE Transactions on Electrical Insulation, Vol. EI-17, No. 6, Dec 1982, p. 488.

12. Klein, N. "Mechanism of Electrical Breakdown in Thin Insulators - An Open Subject," Thin Solid Films, 100, 1983, pp. 335-340.

REFERENCES (Cont.)

13. Ridley, B. K., "Mechanisms of Electrical Breakdown in $SiO_2$ Films," Journal of Applied Physics, Vol. 46, No. 3, Mar 1975, p. 998.

14. von Hippel, A., "Electric Breakdown of Solid and Liquid Insulators," Journal of Applied Physics, Vol. 8, Dec 1937, p. 815.

15. "Standard Test Method for Dielectric Breakdown Voltage and Dielectric Strength of Solid Electrical Insulating Materials Under Direct-Voltage Stress," Designation D3755-79, 1985 Annual Book of ASTRA Standards, Vol. 10.2, p. 554.

16. Laurent, C.; Mayoux, C.; and Sergent, A., "Electrical Breakdown Due to Discharges in Different Types of Insulation," IEEE Transactions on Electrical Insulation, Vol. EI-16, No. 1, Feb 1981, p. 52.

17. Burnley, K. G.; Phil, M.; and Exon, J. L. T., "Relationship between various measurement techniques for void discharges," IEEE Proceedings, Vol. 129, Part A, No. 8, Nov 1982, p. 593.

18. Laurent, C.; Mayoux, C.; and Noel, S., "Dielectric Breakdown of Polyethylene in Divergent Field: Role of Dissolved Gases and Electroluminescence," Journal of Applied Physics, Vol. 54, No. 3, Mar 1983, p. 1532.

19. Tanaka, J. and Greenwood, A., "Effects of Charge Injection and Extraction on Tree Initiation in Polyethylene," IEEE Transactions on Power Apparatus and Systems, Vol. PAS-97, No. 5, Sep/Oct 1978, p. 1749.

20. O'Dwyer, J. J., "Theory of High Field Conduction in a Dielectric," Journal of Applied Physics, Vol. 40, No. 10, Sep 1969, p. 3887.

21. O'Dwyer, J. J., "Breakdown in Solid Dielectrics," IEEE Transactions on Electrical Insulation, Vol. EI-17, No. 6, Dec 1982, p. 481.

22. Kao, K. C., "New Theory of Electrical Discharge and Breakdown in Low Mobility Condensed Insulators," Journal of Applied Physics, Vol. 55, No. 3, Feb 1984, p. 752.

23. "Standard Test Method for Thermal Failure Under Electric Stress of Solid Electrical Insulating Material," Designation D3151-79, 1985 Annual Book of ASTRA Standards, Vol. 10.2, p. 404.

24. Epoxy EN7, Conap, Inc., 1405 Buffalo St., Olean, NY 14760.

25. RTV 615, General Electric, Silicone Products Division, Waterford NY, 12188.

26. RTV 3145, Dow Corning Corporation, Midland, Michigan 48640.

27. Dobratz, B. M., LLNL Explosives Handbook - Properties of Chemical Explosives and Explosive Simulants, Lawrence Livermore National Laboratory, 16 Mar 1981.

REFERENCES (Cont.)

28. Forbes, J. W.; Watt, J. W.; Roslund, L. A.; and Coleburn, N. L., Sensitivity and Performance of Several Selected Insensitive Plastic Bonded Explosives, NSWC TR 83-74, Naval Surface Weapons Center, 1983.

29. EPON 815 Resin, Miller Stephenson Chemical Co., Inc., P. O. Box 950, Danbury, CT 06813.

30. Ancamine T-1 Hardener, Pacific Anchor Chemical Corporation, 6055 East Washington Blvd, Suite 700, Los Angeles, CA 90040.

31. Conversations with R. Dougle, University of South Carolina, Electrical and Computer Engineering Department, Columbia, SC 29208.

32. Sudarshan, T. S.; Nagabushana, G. R.; Thompson, J. E.; Salisbury, K.; and Park, L. R., "Electrostatic Field Evaluation by the Electrolytic Tank Method," Proceedings of the Third International Symposium on Gaseous Dielectrics, Mar 1982, p. 374.

# APPENDIX A

## MODIFICATION OF ELECTRIC FIELD AT DIELECTRIC BOUNDARIES

The object of this appendix is to discuss in more detail how the electric field is modified at the boundary of two differing dielectric constants. If the electric field should pass from a material 1 to a material 2 with a different dielectric constant, ($\varepsilon_{r1} \neq \varepsilon_{r2}$) the field can be modified locally at the boundary. Consider such a system depicted in Figure A-1. The electric field on both sides of the boundary can be broken up into component vectors: the field tangential to the boundary, $E_t$, and the field normal to the boundary, $E_n$. Now the question becomes: how are these component vectors affected by the change in dielectric constant?

The affect on the tangential field can be determined by integrating the field around a closed loop of length $\Delta\ell$ starting on one side of the boundary and returning on the other side as indicated in Figure A-1. Since there is no net work performed on a charge moved around a closed loop, the integral is

$$\oint \overline{E} \cdot \overline{dl} = E_{t1}\ \Delta\ell - E_{t2}\Delta\ell = 0$$

Therefore,

$$E_{t1} = E_{t2}$$

So the tangential fields are equal on both sides of the boundary.

The normal field can be determined by constructing a cylindrical pill box bisected by the boundary with an infinitesimal surface area $\Delta s$ (Figure A-2). The electric field lines can be imagined to flow through the pill box, giving rise to an electric flux density D on both sides of the pill box. The electric flux density is sometimes referred to as the displacement vector and defined as

$$\overline{D} = \varepsilon\overline{E}$$

Now, Gauss's Law states that the flux out of a surface is equal to the total charge inside the volume enclosed by that surface.

$$\int \overline{D} \cdot \overline{ds} = \int_v \rho dv$$

For the surface of Figure A-2 the flux out of the pill box equals $\rho_s \Delta s$. Therefore,

$$D_{n1}\ \Delta s - D_{n2}\ \Delta s = \rho_s \Delta s$$

If the surface has no charge then

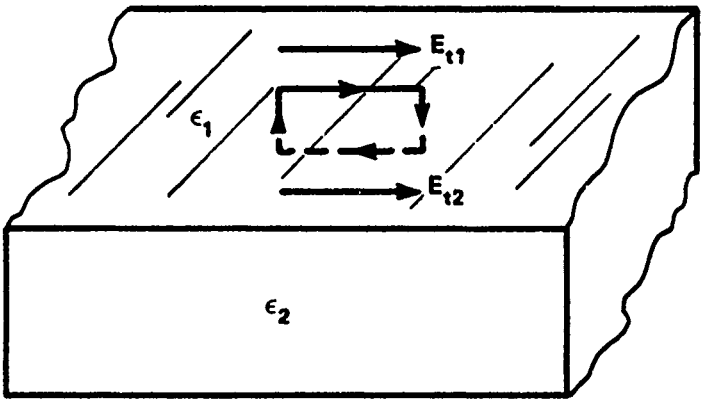


FIGURE A-1. TANGENTIAL FIELD AT DIELECTRIC BOUNDARY

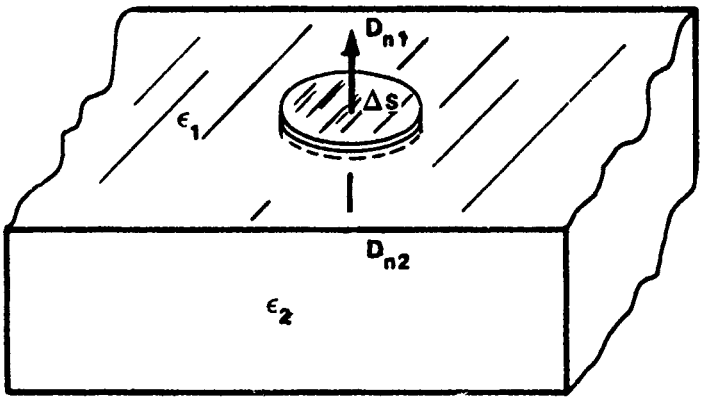


FIGURE A-2. NORMAL FIELD AT DIELECTIC BOUNDARY

$$D_{n1} = D_{n2}$$

and

$$\varepsilon_1 E_{n1} = \varepsilon_2 E_{n2}$$

or

$$E_{n1} = \frac{\varepsilon_2}{\varepsilon_1} E_{n2}$$

Therefore, the electric fields normal to the boundary differ by the ratio of the relative dielectric constants. The resultant field on both sides of the boundary can differ in magnitude and direction depending on the dielectric mismatch.

Now consider a triple junction where a metallic electrode is placed on top of the dielectric boundary. The dielectric mismatch is between the air where $\varepsilon_r$(air) = 1, and the insulating spacer where $\varepsilon_r$(Ins)>1. In SI units, the ratio is numerically equal to $\varepsilon_r$(Ins). For the case presented here and shown in Figure 3-1, there are two items to keep in mind: It has been shown by field plots produced from electrolytic tank measurements that the maximum enhancement is in the low $\varepsilon$ region.[32] Also, at the triple junction where the electrode edge is rounded, the normal field is the dominant constituent of the electric field vector. Consequently, the field at the triple junction can be enhanced by a factor close to the maximum, $\varepsilon_r$(Ins.).

The enhancement of the field at the triple junction can cause external partial discharges (corona) to occur between the high voltage electrode and the insulator. The corona activity starting below the normal partial discharge inception level can cause breakdown to occur in the divergent field below the expected value which is clearly undesirable.

DISTRIBUTION

| | Copies |
|---|---|
| Commander | |
| Naval Air Systems Command | |
| Attn: AIR-350 (H. Benefiel) | 1 |
| AIR-440 (G. Heiche) | 1 |
| AIR-54131 (W. Zuke) | 1 |
| AIR-54131 (R. Jaramillo) | 1 |
| AIR-00D4 (Library) | 1 |
| Department of the Navy | |
| Washington, DC 20361 | |
| Commander | |
| Naval Sea Systems Command | |
| Attn: PMS-400M | 1 |
| SEA-06H3 | 1 |
| SEA-09B312 | 1 |
| SEA-63R (F. Romano) | 1 |
| SEA-62R32 (G. Edwards) | 1 |
| SEA-62YB | 1 |
| SEA-62Y13C | 1 |
| SEA-62Z | 1 |
| SEA-62Z31E | 1 |
| SEA-64E | 1 |
| Department of the Navy | |
| Washington, DC 20362 | |
| Chief of Naval Research | |
| Attn: ONR-1132P (R. Miller) | 1 |
| ONR-260 (D. Seigel) | 1 |
| ONR-400 (J. Satkowski) | 1 |
| ONR-412 (R. Junker) | 1 |
| ONR-741 (Technical Library) | 1 |
| Department of the Navy | |
| Arlington, VA 22217 | |
| Defense Technical Information Center | |
| Cameron Station | |
| Alexandria, VA 22304-6145 | 12 |

| | Copies |
|---|---|
| Commander | |
| Naval Weapons Center | |
| Attn: Technical Library | 1 |
| Code 3835 (R. G. Sewell) | 1 |
| Code 3205 (J. Bryant) | 1 |
| Code 3262 (G. Greene) | 1 |
| Code 3265 (T. Joyner) | 1 |
| Code 385 (A. Amster) | 1 |
| Code 01T (E. Royce) | 1 |
| Code 3891 (D. Mallroy) | 1 |
| Code 3891 (K. Graham) | 1 |
| Code 3895 (K. Kraeutle) | 1 |
| Code 3891 (J. Covino) | 1 |
| China Lake, CA 93555 | |
| Director | |
| Naval Research Laboratory | |
| Attn: J. Aviles | 1 |
| J. Ford (B. 704T) | 1 |
| A. Stolovy | 1 |
| I. Vitkovitsky (B. 71) | 1 |
| Technical Information Section | 2 |
| Washington, DC 20375 | |
| Director | |
| Defense Advanced Research Projects Agency | |
| Attn: H. D. Fair | 1 |
| P. Kemmey | 1 |
| J. Entzminger | 1 |
| Library | 1 |
| Washington, DC 20301 | |
| Commanding Officer | |
| Naval Weapons Station | |
| Attn: R & D Division | 1 |
| L. Rothstein | 1 |
| Yorktown, VA 23691 | |

DISTRIBUTION (Cont.)

| | Copies |
|---|---|
| Air Force Office of Scientific Research | |
| Attn: Col. R. Detweiler | 1 |
| Col. H. Bryan | 1 |
| T. Walsh | 1 |
| Library | 1 |
| Bolling Air Force Base | |
| Washington, DC 20332 | |
| Superintendent | |
| Naval Postgraduate School | |
| Attn: Library | 1 |
| Monterey, CA 93940 | |
| Commanding Officer | |
| Harry Diamond Laboratories | |
| Attn: Library | 1 |
| R. K. Warner | 1 |
| R. Garver | 1 |
| W. Gray | 1 |
| W. Petty | 1 |
| 2800 Powder Mill Road | |
| Adelphi, MD 20783 | |
| Commander | |
| Naval Intelligence Support Center | |
| Attn: NISC-30 | 1 |
| 4301 Suitland Road | |
| Washington, DC 20390 | |
| Chief of Naval Material | |
| Attn: PM-23 (J. Amlie) | 1 |
| MAT-071 (O. Remson) | 1 |
| MAT-0716 (A. Faulstich) | 1 |
| Washington, DC 20362 | |
| Commanding Officer | |
| Naval Ordnance Station | |
| Attn: Research and Development Department | 1 |
| Technical Library | 1 |
| Indian Head, MD 20640 | |

| | Copies |
|---|---|
| Commanding Officer | |
| Ballistics Research Laboratory | |
| USARRADCOM | |
| Attn: Technical Library | 1 |
| R. Frey | 1 |
| F. Grace | 1 |
| P. Howe | 1 |
| R. Jamieson | 1 |
| H. Reeves | 1 |
| J. Starkenberg | 1 |
| W. Walters | 1 |
| Aberdeen Proving Ground | |
| Aberdeen, MD 21005 | |
| Air Force Armament Test Laboratory | |
| Attn: DLYV (A. Rutland) | 1 |
| DLDE (L. Elkins) | 1 |
| DLJW (R. McGuire) | 1 |
| Eglin Air Force Base, FL 32541 | |
| Director | |
| Office of Naval Technology | |
| Attn: E. Zimet | 1 |
| Arlington, VA 22217 | |
| Director | |
| Army Material Systems Analysis Agency | |
| Attn: DRXSY-D | 1 |
| DRXSY-J (J. McCarthy) | 1 |
| Aberdeen Proving Ground | |
| Aberdeen, MD 21005 | |
| Commander | |
| Air Force Armament Development and Test Center | |
| Attn: Lt. Col. Scott | 1 |
| Eglin Air Force Base, FL 32542 | |
| Commanding Officer | |
| Aberdeen Research and Development Center | |
| Attn: Technical Library | 1 |
| Aberdeen, MD 21005 | |

DISTRIBUTION (Cont.)

| | Copies |
|---|---|
| Commanding Officer | |
| U. S. Army Armament Research and Development Center | |
| Attn: F. Owens | 1 |
| N. Slagg | 1 |
| R. Walker | 1 |
| Technical Library | 1 |
| Dover, NJ 07801 | |
| Lawrence Livermore National Laboratory | |
| Attn: L. Green | 1 |
| M. Finger | 1 |
| B. Hayes | 1 |
| H. Kruger | 1 |
| N. Keeler | 1 |
| E. Lee | 1 |
| R. McGuire | 1 |
| P. Urtiew | 1 |
| W. Von Holle | 1 |
| Livermore, CA 94550 | |
| Director | |
| Los Alamos National Laboratory | |
| Attn: G. Andrews (M-9) | 1 |
| M. Butner | 1 |
| W. Davis (M-9) | 1 |
| C. Max Fowler (M-6) | 1 |
| T. Frank | 1 |
| D. Erickson (M-6) | 1 |
| M. Ginsberg (M-8) | 1 |
| J. Goforth (M-6) | 1 |
| T. McDonald | 1 |
| R. Rabie (M-9) | 1 |
| R. Rogers | 1 |
| J. Shaner (M-6) | 1 |
| G. Wackerly | 1 |
| J. Dick | 1 |
| M. Urizar | 1 |
| Technical Library | 1 |
| Los Alamos, NM 87544 | |

| | Copies |
|---|---|
| Director | |
| Johns-Hopkins Applied Physics Laboratory | |
| Attn: S. Koslov | 1 |
| Technical Library | 1 |
| J. Warren, 1W-201 | 1 |
| S. Gearhart, 1E-103 | 1 |
| Johns-Hopkins Road | |
| Laurel, MD 20707 | |
| University of Maryland | |
| Attn: Plasma Physics Dept. | 1 |
| H. Griem | 1 |
| Technical Library | 1 |
| College Park, MD 20740 | |
| SRI International | |
| 333 Ravenswood | |
| Attn: M. Cowperthwaite | 1 |
| Menlo Park, CA 94025 | |
| Texas Technical University | |
| Attn: M. Kristiansen | 1 |
| Department of Electrical Engineering | |
| Lubbock, Texas 79409 | |
| AAI Corporation | |
| Attn: E. P. Connell | 1 |
| P.O. Box 6767 | |
| Baltimore, MD 21204 | |
| ARTEC Associates, Inc. | |
| Attn: R. Barry Ashby | 1 |
| S. P. Gill | 1 |
| 26046 Landing Road | |
| Haywood, CA 94545 | |
| F. J. Seiler Research Laboratory | |
| Attn: Col. B. Loving | 1 |
| U. S. Air Force Academy | |
| Colorado Springs, CO 80840 | |
| Battelle Research Institute | |
| Attn: J. Backofen | 1 |
| Columbus Laboratories | |
| 505 King Avenue | |
| Columbus, OH 43201 | |

DISTRIBUTION (Cont.)

| | Copies |
|---|---|
| Scientific Research Associates, Incorporated<br>Attn: B. Weinberg<br>P. O. Box 498<br>Glastenbury, CT 06033 | 1 |
| Science Applications<br>Attn: W. Chadsey<br>8330 Old Courthouse Road<br>Suite 510<br>Vienna, VA 22180 | 1 |
| Director<br>Sandia National Laboratories<br>Attn: D. Hayes<br>J. Kennedy<br>R. E. Setchell<br>P. L. Stanton<br>Technical Library<br>P. O. Box 5800<br>Albuquerque, NM 87115 | 1<br>1<br>1<br>1<br>1 |
| Honeywell Defense<br>Attn: P. DiBona<br>600 2nd Street N.<br>Hopkins, NM 55343 | 1 |
| Library of Congress<br>Attn: Gift and Exchange Division<br>Washington, DC 20540 | 4 |
| Maxwell Laboratories, Inc.<br>Attn: J. Devoss<br>P. Elliot<br>8835 Balboa Avenue<br>San Diego, CA 92123 | 1<br>1 |
| Department of Electrical Engineering<br>Bell Hall<br>Attn: A. Gilmour, Jr.<br>State University of New York at Buffalo<br>Buffalo, NY 14214 | 1 |
| Georgia Institute fo Technology<br>Georgia Tech. EES; RAIL/RED<br>Attn: D. Ladd<br>Atlanta, GA 30332 | 1 |
| AVCO Everett Research Laboratory<br>Attn: C. Pike<br>2385 Revere Beach Parkway<br>Everett, MA 02149 | 1 |
| Physics Internation Company<br>Attn: J. N. Benford<br>R. F. Johnson<br>A. Rutherford<br>2700 Merced Street<br>San Leandro, CA 94577 | 1<br>1<br>1 |
| Enig Associates<br>Attn: J. Enig<br>13230 Ingleside Drive<br>Beltsville, MD 20705 | 1 |
| Science Applications International Corporation<br>Attn: E. T. Toton<br>1710 Goodridge Drive<br>McLean, VA 22102 | 1 |
| Zernow Technical Services, Inc.<br>Attn: L. Zernow<br>425 W. Bonita Avenue<br>Suite 208<br>San Dimas, CA 91773 | 1 |
| CETR<br>New Mexico Tech.<br>Attn: Anders Persson<br>Socorro, NM 87801 | 1 |
| British Embassy<br>British Defence Staff<br>3100 Massachusetts Ave., N.W.<br>Washington, DC 20008 | 1 |
| Royal Ordnance Ammunition<br>Attn: P. R. Lee<br>Euxton Lane<br>Euxton, Chorley, Lancs.,<br>PR7 GAD, UK | 1 |

DISTRIBUTION (Cont.)

| | Copies |
|---|---|
| Atomic Weapons Research Establishment | |
| Attn: C. Beck | 1 |
| G. Coley | 1 |
| G. Eden | 1 |
| G. Foan | 1 |
| D. Grief | 1 |
| C. Hutchinson | 1 |
| Aldermaston, Reading, BERKS, RG7 4PR, UK | |
| Atomic Weapons Research Establishment | |
| Attn: H. R. James | 1 |
| Foulness Island, Southend-on-Sea Essex, UK | |
| Royal Armament Research and Development Establishment | |
| Attn: J. Connor | 1 |
| I. Cullis | 1 |
| P. Haskins | 1 |
| G. Hooper | 1 |
| M. Nash | 1 |
| Fort Halstead Sevenoaks, Kent, UK | |
| Royal Armament Research and Development Establishment | |
| Attn: K. Bascombe | 1 |
| J. Jenkins | 1 |
| D. Mullenger | 1 |
| A. Owen | 1 |
| B. Hammant | 1 |
| A. Kosecki | 1 |
| Waltham Abbey, Powdermill Lane Essex, EN9 LBP | |
| Defense Research Information Center | |
| Attn: Technical Library | 1 |
| St. Mary Cray, Kent, UK | |
| University of Wales, Aberystwyth | |
| Attn: H. Edwards | 1 |
| G. Thomas | 1 |
| Department of Physics Wales, UK | |

| | Copies |
|---|---|
| Washington State University | |
| Attn: R. Fowles | 1 |
| Y. Gupta | 1 |
| G. Duvall | 1 |
| Pullman, WA 99164 | |
| Oak Ridge National Laboratory | |
| Attn: O. H. Crawford | 1 |
| P. O. Box X | |
| Oak Ridge, TN 37831 | |
| Hercules Aerospace | |
| Attn: M. Klakken | 1 |
| L. Losee | 1 |
| Bacchus Works Magna, Utah 84044 | |
| U. S. Army Missile Command | |
| Attn: D. Dreitzler | 1 |
| J. Knaur | 1 |
| J. Crawford | 1 |
| Redstone Arsenal, AL 35898-5249 | |
| University of South Carolina | |
| Attn: T. Sudarsha | 1 |
| R. Dougle | 1 |
| ECE Dept. Columbia, SC 29208 | |
| Internal Distribution: | |
| E231 | 2 |
| E232 | 15 |
| E23 (W. Smith) | 1 |
| F (R. T. Ryland) | 1 |
| F53 (E. Nolting) | 1 |
| G13 (D. Dickinson) | 1 |
| G22 (D. Brunson) | 1 |
| (W. Mock) | 1 |
| (S. Waggener) | 1 |
| H12 (M. Guthrie) | 1 |
| H23 (E. Nolting) | 1 |
| R10A | 1 |
| R10B | 1 |
| R10C | 1 |
| R10D | 1 |
| R10F | 1 |
| R11 | 1 |
| R11 (T. Hall) | 1 |
| (E. Anderson) | 1 |
| R12 | 1 |

DISTRIBUTION (Cont.)

| | | Copies |
|---|---|---|
| R12 | (J. Erkman) | 1 |
| | (W. Filler) | 1 |
| | (L. Montesi) | 1 |
| | (O. Dengel) | 1 |
| | (P. Spahn) | 1 |
| R13 | | 1 |
| R13 | (R. D. Bardo) | 1 |
| | (A. R. Clairmont) | 1 |
| | (C. S. Coffey) | 1 |
| | (D. L. Demske) | 1 |
| | (W. L. Elban) | 1 |
| | (J. W. Forbes) | 1 |
| | (B. C. Glancy) | 1 |
| | (R. Granholm) | 1 |
| | (H. D. Jones) | 1 |
| | (P. Gustavson) | 1 |
| | (K. Kim) | 1 |
| | (E. R. Lemar) | 1 |
| | (R. J. Lee) | 10 |
| | (T. P. Liddiard) | 1 |
| | (P. J. Miller) | 1 |
| | (C. Richmond) | 1 |
| | (H. W. Sandusky) | 1 |
| | (G. Sutherland) | 1 |
| | (D. G. Tasker) | 1 |
| | (J. W. Watt) | 1 |
| | (F. J. Zerilli) | 1 |
| R14 | | 1 |
| R14 | (J. Gaspin) | 1 |
| | (D. O'Keeffe) | 1 |
| | (D. Lehto) | 1 |
| R15 | | 1 |
| R15 | (W. Faux) | 1 |
| | (R. Tussing) | 1 |
| R16 | | 1 |
| R34 | (J. Sharma) | 1 |
| R41 | (M. Cha) | 1 |
| | (H. Uhm) | 1 |
| R401 | | 1 |